

Technical Report No. 32-641

# *The Absolute Spectral-Energy Distribution of Canopus*

*R. H. Norton*

64 32995  
(ACCESSION NUMBER)  
34  
(PAGES)  
CR-59162  
(NASA CR OR TMX OR AD NUMBER)

(THRU)  
7  
(CODE)  
88  
(CATEGORY)



JET PROPULSION LABORATORY  
CALIFORNIA INSTITUTE OF TECHNOLOGY  
PASADENA, CALIFORNIA

August 15, 1964

OTS PRICE

XEROX

\$

2.00 FS

MICROFILM

\$

0.50 mf.

*Technical Report No. 32-641*

*The Absolute Spectral-Energy Distribution  
of Canopus*

*R. H. Norton*

*Norri Sirri*

Norri Sirri, Chief

Guidance and Control Research Section

JET PROPULSION LABORATORY  
CALIFORNIA INSTITUTE OF TECHNOLOGY  
PASADENA, CALIFORNIA

August 15, 1964

**Copyright © 1964  
Jet Propulsion Laboratory  
California Institute of Technology**

**Prepared Under Contract No. NAS 7-100  
National Aeronautics & Space Administration**

## CONTENTS

I. Introduction . . . . .	1
II. Stellar Spectrophotometry . . . . .	2
III. Observations Made Prior to 1960 . . . . .	3
IV. Present Work . . . . .	5
V. Calibration to Absolute Units . . . . .	13
VI. Future Plans . . . . .	16
Nomenclature . . . . .	16
References . . . . .	17
Appendices:	
A. Computational Procedures and Network Reduction Equations . . .	18
B. Reproductions of Actual Scanner Tracings . . . . .	21

## TABLES

1. Derived extinction coefficients . . . . .	8
2. Possible standard stars . . . . .	9
3. Assumed relative SED of $\xi^2$ Ceti . . . . .	10
4. Smoothed relative SED . . . . .	11
5. Relative SED of Canopus . . . . .	13
6. The Johnson <i>UBV</i> bandpasses . . . . .	14
7. <i>UBV</i> magnitudes of Vega and Canopus . . . . .	15
8. Parameters of model atmosphere for Canopus . . . . .	15

## FIGURES

1. Comparison of monochromatic magnitude system of Code and Woolley . . . . .	4
2. Comparison of Willstrop and Code . . . . .	4

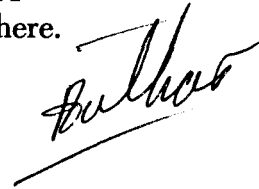
**FIGURES (Cont'd)**

3. Preliminary SED of Canopus . . . . .	4
4. Reproduction of actual scanner tracing of Canopus . . . . .	6
5. Monochromatic extinction curves . . . . .	7
6. Typical fit to a modified Rayleigh law . . . . .	7
7. Network of links showing stars in Southern Hemisphere . . . . .	9
8. Assumed SED of $\xi^2$ Ceti . . . . .	10
9. Distribution of errors for $\lambda = 0.437 \mu$ . . . . .	11
10. Variation with wavelength of the standard deviation of a single observation . . . . .	12
11. Line-absorption correction factor for Canopus . . . . .	12
12. Relative SED of Canopus corrected for absorption lines . . . . .	13
13. SED of Canopus . . . . .	15
B-1. Reproduction of actual scanner tracing . . . . .	21
B-2. Reproduction of actual scanner tracing . . . . .	22
B-3. Reproduction of actual scanner tracing . . . . .	23
B-4. Reproduction of actual scanner tracing . . . . .	24
B-5. Reproduction of actual scanner tracing . . . . .	25
B-6. Reproduction of actual scanner tracing . . . . .	26
B-7. Reproduction of actual scanner tracing . . . . .	26
B-8. Reproduction of actual scanner tracing . . . . .	27
B-9. Reproduction of actual scanner tracing . . . . .	28
B-10. Reproduction of actual scanner tracing . . . . .	29
B-11. Reproduction of actual scanner tracing . . . . .	29

**ABSTRACT**

32995

Astronomical observations made by Dr. L. H. Aller and Dr. D. J. Faulkner of the spectral-energy distributions (SED) of twelve stars are presented, including Canopus. Computational procedures for reducing these observations to a system of absolute units of flux outside the Earth's atmosphere are discussed, and the resulting absolute SED are given. Because of its special importance for guidance and control purposes, the SED of Canopus has been corrected for the effect of absorption lines, and the observations have been supplanted in the ultraviolet and infrared by a theoretical model atmosphere.

**I. INTRODUCTION**

The success of interplanetary spacecraft missions depends critically upon precise attitude control of the spacecraft. Two axes of the spacecraft may be controlled by means of optical sensors that detect the Sun. In order to align the spacecraft about the third axis, another object, preferably at right angles to the Sun-spacecraft line, is required. For lunar missions, the Earth may be used. For missions to other planets, it is desirable to use some other celestial object whose brightness and position will not vary so drastically during the mission. A logical choice for this third-axis celestial reference is the star Canopus, since it is the second brightest star in the celestial sphere and is located at high ecliptic latitudes (Ref. 1).

In order to track the star with the spacecraft sensor, the star must first be identified among the background of stars. In the particular case of Canopus, this would seem to be most easily accomplished by means of brightness. Another method that has been proposed is to

measure its color, defined as the ratio of brightnesses through two spectral passbands. A factor which enters heavily into both methods is the absolute spectral-energy distribution (SED), defined as the energy incident outside the Earth's atmosphere as a function of wavelength per unit area per unit wavelength. This information must at the present time be derived from astronomical observations, made of necessity from the Earth's surface.

The purpose of this Report is to summarize the available astronomical observations, to describe the manner in which they are reduced to a desirable form for spacecraft guidance and control purposes, and to present the best absolute SED for Canopus and certain other bright stars.

Section II of this Report contains the background information describing current astronomical methods of obtaining absolute SED. Basic definitions used in later

sections also appear in Section II. Section III summarizes briefly the observations made of Canopus prior to 1960, and the results obtained from them. Section IV describes the most modern and accurate photoelectric observations yet made of 25 bright stars, including Canopus, in the southern celestial sphere, and the manner in which these particular observations were reduced. Calibration to ab-

solute units of all observations described in Sections II, III, and IV is contained in Section V, with the final adopted SED. Finally, Section VI suggests ways and means of improving or implementing the present ground-based observations. Appendix A contains the detailed presentation of the required mathematical derivations that are presented briefly in the text.

## II. STELLAR SPECTROPHOTOMETRY

The term spectrophotometry will be encountered many times in this Report; it means the measurement of the radiant flux from a body as a function of wavelength. In general, there are two types of photometry, wide-band and narrow-band. In the first type, the radiant energy from a star is integrated over several hundred angstroms by a combination of filters and a detector. An example of such a system of photometry is the widely used *UBV* system (Ref. 2). In this system, various filters used in conjunction with a photomultiplier tube isolate spectral passbands up to 1000 Å wide, centered in the *Ultraviolet* (3600 Å), *Blue* (4200 Å), and *Visual* (5400 Å); hence, the abbreviated term *UBV*. It is clear that with spectral passbands many hundreds of angstroms wide, most of the detail in a stellar energy distribution is lost; only the grossest features remain, such as the average slope of the energy distribution on the red side of the observed maximum. In Section V, we will use observations made with this system in order to calibrate our observations to absolute units of flux.

The second type of photometry isolates small spectral regions up to 20 Å wide by means of interference filters, or monochrometers. Obviously, much more information can be obtained about a stellar energy distribution through narrow-band photometry, with which this Report will be mainly concerned.

A class of observation that is popular today, and that falls into the second category above, uses a grating monochrometer at the focus of a large reflecting telescope to isolate small spectral passbands of a few angstroms. The light from a star is focused by the telescope

on the entrance slit of the monochrometer; the monochromatic light, which emerges from the exit slit of the monochrometer, is measured by a photomultiplier tube, and the amplified anode current is displayed on a strip-chart recorder. The grating of the monochrometer is rotatable and is driven by an electric motor. Thus, as the grating is rotated, the spectrum is scanned and a continuous recording of the finer details of a stellar energy distribution is made.

The term absolute SED must be used with care. Wherever it is used in this Report, it means the true observed radiant flux of a star outside the Earth's atmosphere, in  $\text{w/cm}^2/\mu$ . The term relative SED refers to the same radiant flux, but it is normalized to unity either at the peak or at a convenient wavelength. It should be noted that these terms, so defined, differ from the definition in the astronomical literature (Refs. 3 and 4).

Relative monochromatic magnitudes are defined as

$$m(\lambda) = -2.5 \log_{10} \left[ \frac{f(\lambda)}{f(\lambda_0)} \right] \quad (1)$$

where  $f(\lambda)$  is the observed radiant flux at wavelength  $\lambda$ . A second useful definition is that of the spectrophotometric gradient, defined as the monochromatic magnitude difference between two stars at the same wavelength

$$g(\lambda) = m_1(\lambda) - m_2(\lambda) \quad (2)$$

If two stars are observed with the same telescope and detector on the same night, and one of the stars is a standard star whose relative SED is known, it can be seen that we can at once obtain the relative SED of the second star through Eq. 2. In fact, the absolute SED of a standard star is established through Eq. 2, by comparison with a standard lamp whose emissivity is known. For a critical discussion of this problem of establishing a standard star, and for a complete bibliography on the subject, see Ref. 3.

At the present time, the fundamental standard star upon whose SED all other stars are based is Vega ( $\alpha$  Lyrae). In this Report, we assume the relative SED

of Vega given by Code (Ref. 3), and base all observations of Canopus as directly as possible on this distribution. Then, if it should happen that the SED of Vega should require revision, the SED of Canopus, or of any star which has been based on Vega, will require revision by the same amount.

A number of carefully selected, secondary-standard stars have been compared directly with Vega by Code (Ref. 3) and Oke (Ref. 4). These stars will prove to be extremely important, because Canopus and Vega cannot be observed from the same observatory at the same time. Hence, we must choose one of these secondary standards in order to refer observations of Canopus to Vega.

### III. OBSERVATIONS MADE PRIOR TO 1960

The earliest yet modern direct observations of the SED of Canopus that appear in the astronomical literature are those of Woolley, Gascoigne, and de Vaucouleurs (Ref. 5). In their study, an objective-prism spectrograph of 4-in. aperture was used to compare photographically the spectra of 85 bright Southern-Hemisphere stars directly with standard lamps. Because of the nonlinear dispersion of a prism spectrograph, the effective slit-width varied from 20 Å in the blue to 50 Å in the red. In all, 110 photographic plates were measured, each plate containing about 40 spectra. Photographic densities were measured at six wavelengths between 4000 and 6400 Å.

Uncertainties in photographic measurements of this kind are very large; hence an attempt will be made to base Woolley's (*et al.*) relative measurements on the more accurate system of secondary stars established by Code. Two stars on Woolley's list are  $\beta$  and  $\epsilon$  Orionis, stars whose SED have been compared with Vega photoelectrically by Code (Ref. 3). Thus, we may take the relative SED given by Woolley for Canopus, refer it to their SED for  $\beta$  Orionis and  $\epsilon$  Orionis and, eventually, albeit rather indirectly, base Canopus on Vega through the photoelectric data of Code.

Since we have two stars,  $\epsilon$  Orionis and  $\beta$  Orionis, by which the transformation may be made from Woolley's monochromatic magnitudes to the monochromatic magnitudes of Vega, we must check to see if the transformations through the two stars are consistent. The monochromatic magnitudes for  $\epsilon$  Orionis and  $\beta$  Orionis as given by both Code and Woolley are shown in Fig. 1, where an arbitrary zero point at  $\lambda = 0.425 \mu$  has been chosen. It can be seen that a systematic correction as a function of wavelength must be made to the SED given by Woolley if we assume that the SED given by Code are correct. Moreover, this correction seems to be the same for both  $\epsilon$  Orionis and  $\beta$  Orionis. A mean correction was determined from Fig. 1 and applied to the monochromatic magnitudes given for Canopus by Woolley. These monochromatic magnitudes for Canopus were then converted to a relative SED by

$$\frac{f(\lambda)}{f(\lambda_0)} = 10^{-0.4 m(\lambda)} \quad (3)$$

where  $m(\lambda)$  = monochromatic magnitudes of Woolley corrected as described above,  $f(\lambda)/f(\lambda_0)$  = relative SED, normalized to unity at  $\lambda_0 = 0.425 \mu$ .



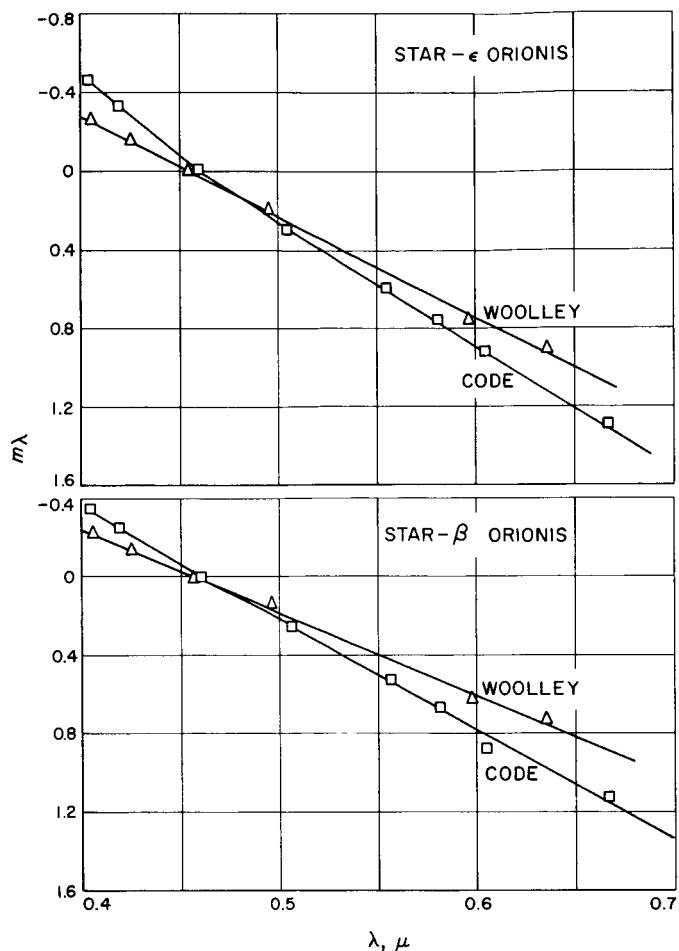


Fig. 1. Comparison of monochromatic magnitude system of Code and Woolley

Observations of somewhat higher reliability were obtained by Willstrop (Ref. 6), using narrow-band interference filters and a photoelectric detector. Willstrop's observations were made at four wavelengths, and the width of his filter bands was about 200 Å. Thus, Willstrop's observations, in a sense, lie between the two extreme types of spectrophotometric observations discussed in Section II. Willstrop also calibrated his observations by means of a standard lamp, but as this calibration was not given, it cannot be used.

To reduce the relative SED given by Willstrop to the system established by Code, the same procedure is followed as for the observations of Woolley. There are six stars common to both Willstrop's and Code's lists. The relative SED as given by Code (Ref. 3) and by Willstrop (Ref. 6), expressed in monochromatic magnitudes through Eq. 1, were plotted for each of the six stars in common. Smooth curves were drawn through Code's points, and

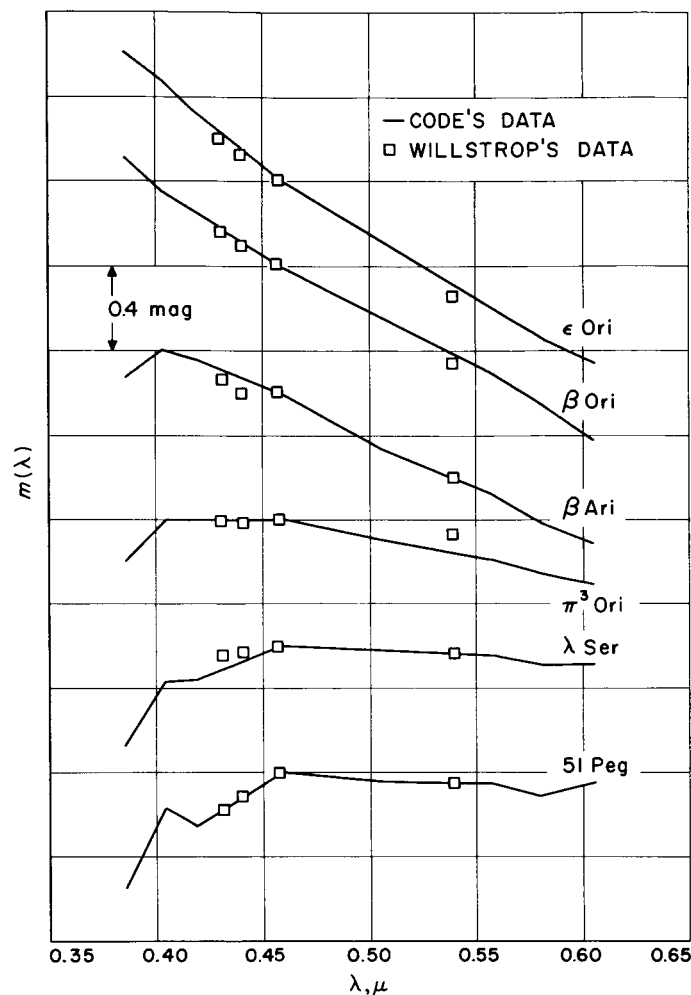


Fig. 2. Comparison of Willstrop and Code

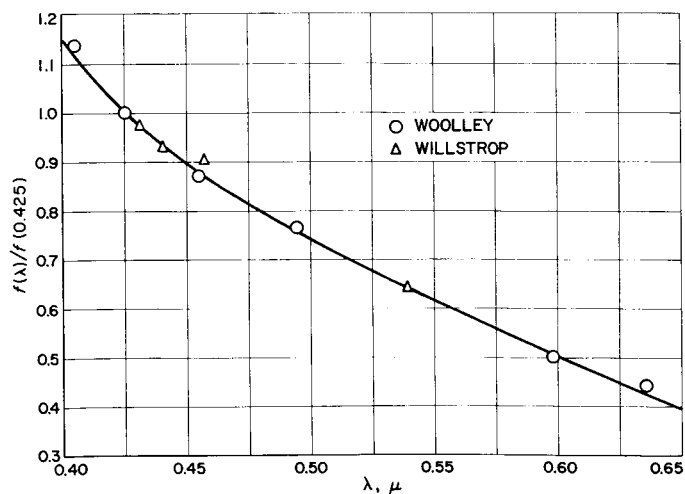


Fig. 3. Preliminary SED of Canopus

mean corrections were derived for each of Willstrop's four passbands. These corrections were then applied to the data supplied by Willstrop for Canopus. Figure 2 shows the agreement between Code's data for the six stars mentioned above and Willstrop's corrected data for the same stars. Figure 3 shows the relative SED of Canopus after smoothing, in which the data supplied by Woolley are represented by circled dots and Willstrop's data are shown by dots within triangles.

Willstrop made no observation at the wavelength which has been chosen (somewhat arbitrarily) to be the reference wavelength for normalization. Therefore, from the best curve which could be fitted through Willstrop's data, a mean normalization constant was determined to make this curve agree as closely as possible with the best

curve which could be fitted through Woolley's data. This curve was derived from the data supplied in magnitudes by the two authors above and transformed to intensity units, through Eq. 3, normalized to unity at  $\lambda = 0.425 \mu$ .

Figure 1 indicates that a systematic difference exists between Woolley's and Code's systems of stellar energy distributions. This difference, however, is the same to within 5% for the two stars in common; but because the work is derived from photographic observations, a rather low weight must be ascribed to it. Willstrop's observations were photoelectric; moreover, there are six stars in common with Code's system. Figure 2 suggests an internal consistency between Willstrop and Code, after adjustment, to  $\pm 4\%$  rms.

#### IV. PRESENT WORK

The most modern and accurate observations of the SED of Canopus were kindly made available by Dr. Lawrence H. Aller and Dr. Donald J. Faulkner,<sup>1</sup> observations made in Australia at the Mt. Stromlo Observatory and its field station at Mt. Bingar. Large reflecting telescopes were used, and a rotating-grating spectrograph scanned each star's spectrum, recording the light intensity at any wavelength through a photomultiplier, current amplifier, and strip-chart recorder.

The general procedure followed in producing such a scanner tracing is now presented. The astronomer takes a dark-current reading, a measure of the noise of the photomultiplier tube. He commences to scan the spectrum of the star. When the scan is completed in one direction, he reverses the gear mechanism of the scanner and records a scan in the reverse direction. Sidereal times are marked at appropriate intervals on the chart, and the amplifier gain is turned up or down, as necessary. Each time a change is made, of course, the new

settings are recorded. One observation thus consists of a deflection measurement on the recorder chart, measured in arbitrary units from the no-signal or dark-current reading of the photomultiplier tube, the amplifier gain, and the sidereal time of the observation. Additional data used in the reduction process are the star's right ascension and declination, and the latitude of the observatory.

A smooth curve is drawn as an upper envelope to the scanner tracing; this curve presumably represents the star's "continuum," or the energy distribution that would be observed if absorption lines were not present. For extremely hot stars, this continuum approaches a true black-body distribution; at lower temperatures, continuous opacity sources, such as atomic hydrogen, helium, and the negative-hydrogen ion, combine to alter the shape of the continuum. Care must be taken at this point to interpret each tracing in a systematic manner, for the continuum on two independent tracings of the same star should be drawn in the same manner relative to the actual scanner tracing. A reproduction of an actual scanner tracing is shown in Fig. 4. Note the relation between

<sup>1</sup>To be published in the astronomical literature by L. H. Aller, D. J. Faulkner and R. H. Norton.

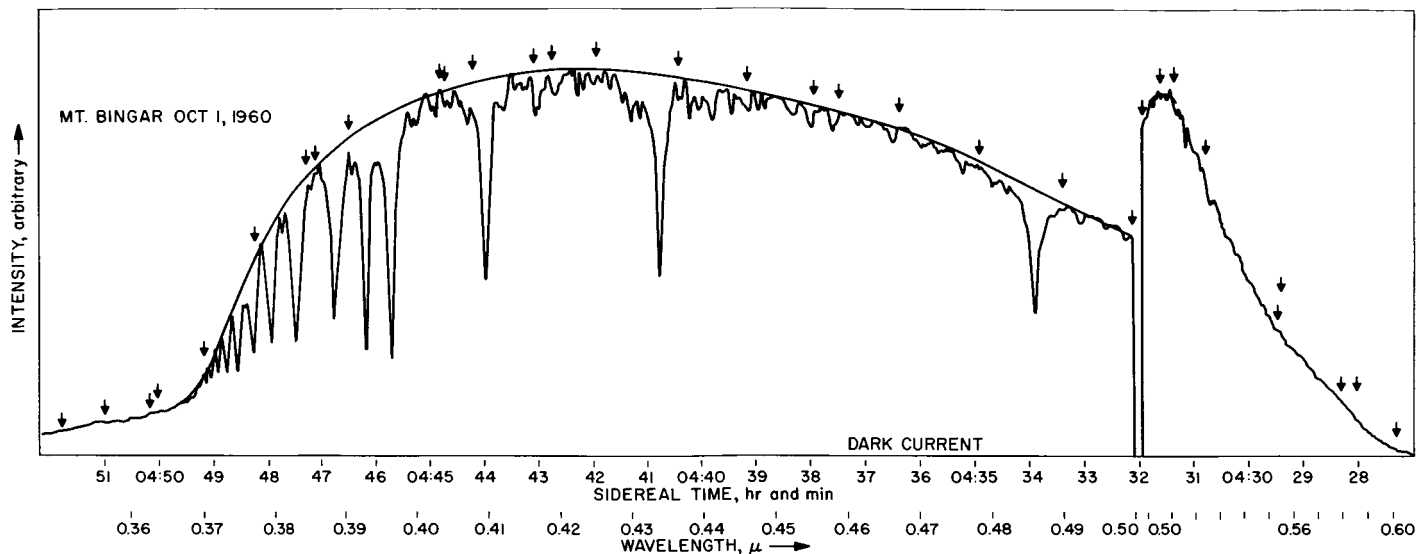


Fig. 4. Reproduction of actual scanner tracing of Canopus

the real stellar energy distribution, which is characterized by deep absorption lines, and the continuum, drawn as a smooth upper envelope to the true energy distribution. Note also the discontinuity at  $\lambda = 0.5 \mu$ . The monochrometer grating was used in the second order, and thus an overlap with ultraviolet light from the third order was found at approximately  $0.5 \mu$ . For this reason, an ultraviolet-blocking filter and a higher amplifier gain were used while scanning wavelengths between  $0.5$  and  $0.6 \mu$ . Later in the program it was found that the filter should have been inserted at about  $0.48 \mu$ ; hence, all observations between  $0.48$  and  $0.50 \mu$  have been discarded. It should be noted that for the purpose of determining the real energy distribution, it does not matter whether this envelope is actually the true stellar continuum or not, for in Section V we will take the absorption lines into account and will deduce the real SED from this smooth curve.

A set of wavelengths are selected in particular spectral regions where no strong absorption lines are present. In this program, 34 such wavelengths were selected. The wavelengths are not equally spaced; yet every spectral region where abrupt changes in the continuum might occur is adequately covered. The locations of the wavelengths at which measurements were made are indicated by short vertical arrows. The deflection measured at each wavelength is the deflection to the continuum, drawn as described above.

The first step in the reduction was the determination of atmospheric extinction. On 25 of the 30 nights, tracings

were made of one or two stars at two or more altitudes as they rose from the horizon to the meridian. Converting the observed light intensity to astronomical magnitudes we have

$$m_{\lambda} = -2.5 \log_{10} d_{\lambda} + \mathcal{G}_{\lambda} \quad (4)$$

where the subscript  $\lambda$  is used to denote an observation at any wavelength. In this Equation,  $d_{\lambda}$  and  $\mathcal{G}_{\lambda}$  are the scanner deflection (in arbitrary intensity units) and an amplifier gain (in magnitudes), respectively.

We account for absorption of light by the Earth's atmosphere in the following manner. Consider a layer of absorbing material of thickness  $dx$  which absorbs a fraction  $\tau dx$  of a monochromatic ray of intensity  $I$ . The amount of the loss is  $I \tau dx$ . In differential form, we have

$$dI = -I \tau dx \quad (5)$$

and integrating over a path length  $x$ , we obtain

$$\log_e I = \log_e I_0 - \tau x \quad (6)$$

where  $I_0$  and  $I$  are the initial and final intensities, respectively. In magnitude form this becomes

$$m_0 = m - 1.086 \tau x \quad (7)$$

$$= m - k X \quad (8)$$

where  $X$  is the path length now expressed in units of the air mass at the zenith of the observer, and the extinction coefficient  $k$  is a measure of the light loss in magnitudes for a star at the zenith. The relative air mass  $X$  in units of the thickness at the zenith is given to a high degree of accuracy by the secant of the zenith angle  $z$ . The error introduced is only 0.005 air mass at  $z = 60$  deg (Ref. 7). A polynomial approximation capable of accuracy exceeding 0.1% up to  $X = 6.8$  and better than 1% up to  $X = 10$  is

$$X = \sec z - 0.0018167 (\sec z - 1) - 0.002875 (\sec z - 1)^2 - 0.0008083 (\sec z - 1)^3 \quad (9)$$

and the value of  $\sec z$  is readily determinable for any observation through the relation

$$\sec z = (\sin \phi \sin \delta + \cos \phi \cos \delta \cos h)^{-1} \quad (10)$$

where  $\phi$  is the observer's latitude, and  $\delta$  and  $h$  are the declination and hour angle, respectively, of the star.

Denoting, as before, an observation at a particular wavelength by a subscript  $\lambda$ , Eq. 8 becomes

$$m_\lambda(X_\lambda) = m_\lambda^0 + k_\lambda X_\lambda \quad (11)$$

where the superscript zero denotes a quantity observed outside the Earth's atmosphere. On a given night,  $k_\lambda$  is obtained by a least-squares fit over  $X_\lambda$  for each  $\lambda$ ; since the main source of atmospheric extinction is Rayleigh scattering, we fit these  $k_\lambda$  to a modified  $\lambda^{-4}$  law

$$k_\lambda = a + b \lambda^{-4} \quad (12)$$

The constant term  $a$  allows for extinction from any dust or haze that might be present in the atmosphere. Such a source of extinction, of course, does not affect the shape of the SED. Figure 5 illustrates some typical extinction data, showing  $m_\lambda$  as a function of  $X_\lambda$  for several wavelengths. In Fig. 6, a typical fit is shown to a modified Rayleigh law, where  $k_\lambda$  is plotted against  $\lambda^{-4}$ .

Extinction coefficients were not measured on five of the nights; hence, the results of the other 25 were grouped and averaged. Table 1 gives the values determined, the grouping and the mean extinction coefficients adopted, and the associated standard errors (1  $\sigma$  rms).

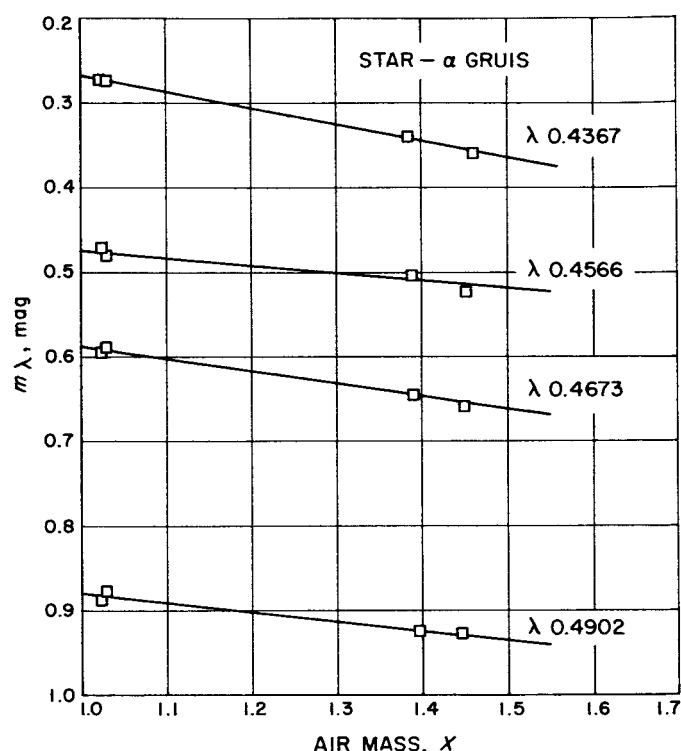


Fig. 5. Monochromatic extinction curves

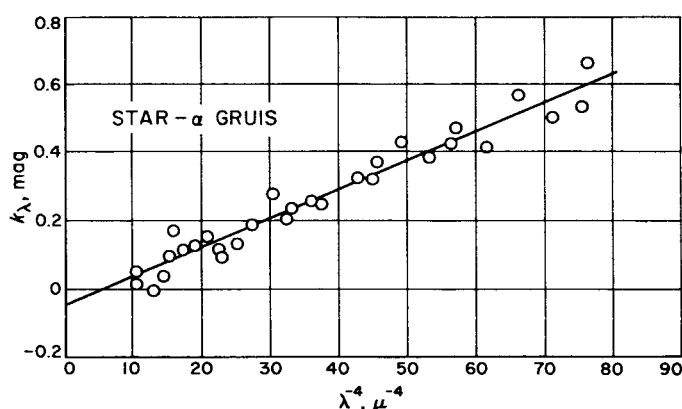


Fig. 6. Typical fit to a modified Rayleigh law

While on the surface the errors reported in Table 1 would suggest that the extinction coefficients are poorly determined, in actuality they affect the SED very little. To show this, we write the monochromatic magnitudes for two stars, 1 and 2

$$\begin{aligned} m_i^0(\lambda) &= m_{i\lambda} - m_{i\lambda_0} - k_\lambda X_{i\lambda} + k_{\lambda_0} X_{i\lambda_0} \quad (13) \\ &= m_{i\lambda} - m_{i\lambda_0} - a (X_{i\lambda} - X_{i\lambda_0}) \end{aligned}$$

$$-b \left( \frac{X_{1\lambda}}{\lambda^4} - \frac{X_{1\lambda_0}}{\lambda_0^4} \right) \quad (14)$$

$$m_2^0(\lambda) = m_{2\lambda} - m_{2\lambda_0} - a(X_{2\lambda} - X_{2\lambda_0}) - b \left( \frac{X_{1\lambda}}{\lambda^4} - \frac{X_{1\lambda_0}}{\lambda_0^4} \right) \quad (15)$$

Table 1. Derived extinction coefficients<sup>a</sup>

Date	Observatory	$a$	$b$	Adopted means
(1960)				
Aug 24	Mt. Stromlo	—	—	
Aug 25	↓	0.278	0.008507	
Aug 26		-0.030	0.007737	$a = 0.079 \pm 0.040$
Aug 28		0.140	0.009954	
Aug 30		0.089	0.011597	$b = 0.00965 \pm 0.00090$
Aug 31		—	—	
Sept 20	↓	—	—	
Sept 28	Mt. Bingar	-0.081	0.009015	
Oct 1	↓	-0.011	0.007317	
Oct 12		0.154	0.007579	
Oct 14		0.085	0.007363	$a = 0.042 \pm 0.030$
Oct 15		0.008	0.010226	
Oct 16		—	—	
Oct 19		0.040	0.010983	$b = 0.00859 \pm 0.00070$
Oct 22		0.368	0.008624	
Nov 5		0.107	0.007565	
Nov 6		0.035	0.009749	
Nov 9	↓	0.038	0.007442	
(1961)				
Jan 9	Mt. Bingar	0.168	0.015033	$a = 0.148 \pm 0.08$
Jan 13	↓	0.129	0.008929	$b = 0.0089 \pm 0.0009$
Jan 14		—	—	
Jan 17	Mt. Stromlo	0.076	0.007621	
Mar 8	Mt. Bingar	0.144	0.011852	
Mar 9	↓	0.083	0.008231	
Mar 10		-0.110	0.012264	
Mar 11		-0.086	0.009293	
Mar 15		-0.021	0.010122	
Mar 16	↓	-0.014	0.010744	
Mar 22	Mt. Stromlo	0.119	0.007954	
May 5	Mt. Stromlo	0.011	0.009002	

<sup>a</sup> Nights on which extinction coefficients were not measured are indicated in columns 3 and 4 by a "—". For groups in which no "—" appears, no adopted means are required.

The spectrophotometric gradient between these two stars is defined in Section II. It is

$$g(\lambda) = m_1^0(\lambda) - m_2^0(\lambda) = [m_{1\lambda} - m_{2\lambda} - m_{1\lambda_0} + m_{2\lambda_0}] - a[X_{1\lambda} - X_{1\lambda_0} - X_{2\lambda} + X_{2\lambda_0}] - b \left[ \frac{X_{1\lambda} - X_{2\lambda}}{\lambda^4} - \frac{X_{1\lambda_0} - X_{2\lambda_0}}{\lambda_0^4} \right] \quad (16)$$

Performing a variation on  $a$  and  $b$ , we have

$$\delta g(\lambda) = -[X_{1\lambda} - X_{1\lambda_0} - X_{2\lambda} + X_{2\lambda_0}] \delta a - \left[ \frac{X_{1\lambda} - X_{2\lambda}}{\lambda^4} - \frac{X_{1\lambda_0} - X_{2\lambda_0}}{\lambda_0^4} \right] \delta b \quad (17)$$

A typical scanner tracing is completed in ten minutes or so; thus to a very good approximation

$$X_{1\lambda} \approx X_{1\lambda_0}$$

$$X_{2\lambda} \approx X_{2\lambda_0}$$

and the dominant source of error is in  $\delta b$ .

$$\delta g(\lambda) \approx -(X_{1\lambda_0} - X_{2\lambda_0}) \left( \frac{1}{\lambda^4} - \frac{1}{\lambda_0^4} \right) \delta b \quad (18)$$

In this program,  $1/\lambda_0^4$  is about  $30 \mu^{-4}$ , the maximum  $1/\lambda^4$  can achieve is  $74 \mu^{-4}$ , and  $1.0 \leq X \leq 2.0$ ; hence

$$\delta g(\lambda)_{\max} \approx -44 \delta b \quad (19)$$

Typical values for  $\delta b$  from Table 1 are about  $\pm 0.001$ ; hence

$$\delta g(\lambda)_{\max} \approx \pm 0.04 \text{ mag}$$

In actuality, this error is reduced on the average by a factor of 3 or 4, because as many scanner tracings as possible were obtained with  $X$  close to 1.0, and very few were close to 2.0. The uncertainties introduced into the spectrophotometric gradients on a single night on the basis of a single tracing per star are thus estimated to be  $\pm 0.01$  mag or  $\pm 1\%$ . The contribution of these uncertainties, which are random, to the final SED, which are obtained from averages over many tracings on many nights, is much lower.

The final step in the reduction produces the SED. On each of the 30 nights, there were two to eight stars observed; over the entire observing period of nine months, the entire Southern Celestial Sphere could be observed. Thus, a given star on the list was compared with several other stars. Each comparison is a "link", and the network of links is shown in Fig. 7. Over 30 nights there were 100 such "links"; thus, we have a network of 24 unknown stars, one standard star, and 100 observations linking them. Each "link" is, in reality, a spectrophotometric gradient, which has been discussed. Over-determination is approximately four to one, and a least-squares adjustment becomes appropriate. We follow the procedure of Cohen, Crowe, and Dumond (Ref. 8) in their analysis of the over-determined physical constants. The details of the mathematical analysis are contained in Appendix A.

As has been mentioned, Vega is the fundamental standard star for spectrophotometry. However, Vega

could not be observed from Australia. For this reason, five additional stars were observed, whose SED had been previously determined by as direct a comparison as possible with Vega. These stars and their right ascensions, declinations, visual magnitudes, and spectral types are given in Table 2. The last column gives the source from which each star's relative SED was taken.

Table 2. Possible standard stars

Star	Right ascension,		Declination		V	Spectral type	Source
	hr	min	deg	min			
$\xi^2$ Ceti	2	25	+8	14	4.27	B9 III	Oke <sup>1</sup>
$\beta$ Orionis	5	12	-8	15	0.14	B8 Ia	Code <sup>2</sup>
$\epsilon$ Orionis	5	34	-1	14	1.70	B0 Ia	Code <sup>2</sup>
$\alpha$ Leonis	10	06	+12	13	1.33	B7 V	Oke <sup>1</sup>
58 Aquilae	19	52	+0	08	5.57	A0	Oke <sup>1</sup>

Since the network of southern stars observed by Aller and Faulkner needs only one standard star to be placed on an absolute basis, it was decided to choose one of the stars listed in Table 2 as a secondary standard. If it should prove later that this standard star needs corrections in its energy distribution, each star in the network will need to be corrected by the same amount. This would not be true, however, if the average of the results obtained from more than one standard star were used, and one of those should be in error.

$\xi^2$  Ceti was selected as a standard star for three reasons: (1) it seems, on the surface, to be one of the best observed by Oke; (2) unlike others in Table 2, it was compared *directly* with Vega; and (3) it was one of the stars most often observed in the present program. Figure 8 shows the relative SED of  $\xi^2$  Ceti after Oke<sup>2</sup>, in magnitudes on a  $1/\lambda$  scale. The relation between a  $1/\lambda$  scale and a  $\lambda$  scale is as follows:

$$m(1/\lambda) = -2.5 \log_{10} \left[ \frac{f(1/\lambda)}{f(1/\lambda_0)} \right] \quad (20)$$

$$m(\lambda) = -2.5 \log_{10} \left[ \frac{f(\lambda)}{f(\lambda_0)} \right] \quad (21)$$

Now, since

$$f(\lambda) d\lambda = f(1/\lambda) d(1/\lambda) \quad (22)$$

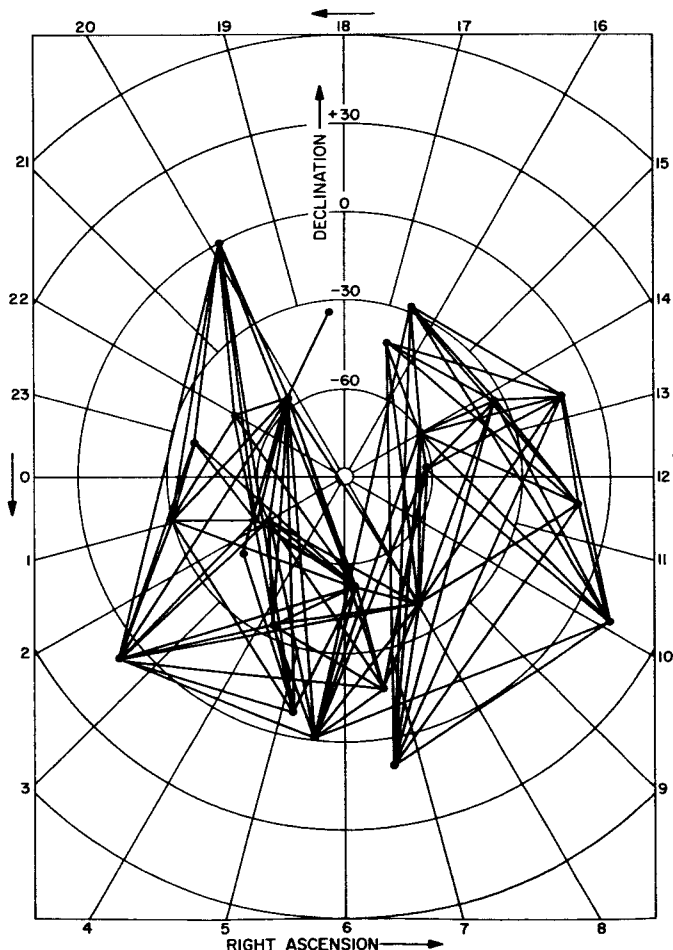
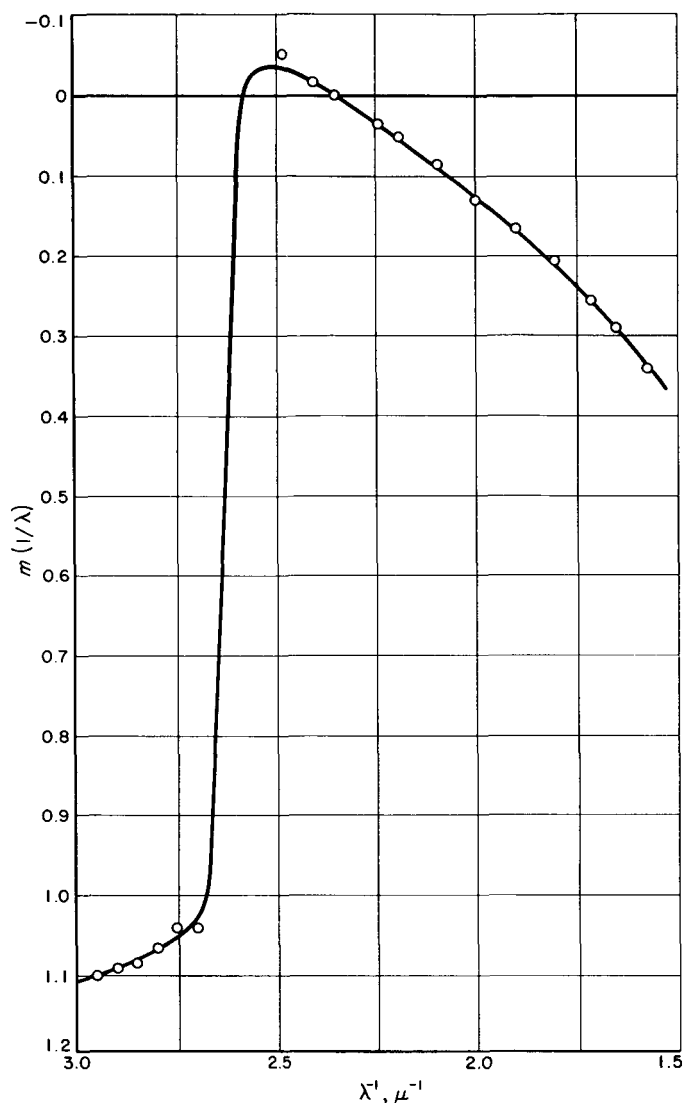


Fig. 7. Network of links showing stars in Southern Hemisphere

<sup>2</sup>Private communication with J. B. Oke, 1964.

Fig. 8. Assumed SED of  $\xi^2$  Ceti

it follows that

$$m(\lambda) = m(1/\lambda) + 5 \log_{10} \left[ \frac{\lambda}{\lambda_0} \right] \quad (23)$$

Figure 8 illustrates the smoothed curve assumed in this Report. Table 3 gives, for the 34 wavelengths adopted in this program, the relative SED of  $\xi^2$  Ceti used in the least-squares reduction of the 25-star network.

Table 4 gives the results of the least-squares reduction for 12 stars in this program brighter than visual magnitude 2.0. It is emphasized that the relative SED in Table 4 refer to a fictitious continuum and not to the true SED.

Table 3. Assumed relative SED of  $\xi^2$  Ceti

$\lambda, \mu$	$1/\lambda, \mu^{-1}$	$m(1/\lambda), \text{mag}$	$m(\lambda), \text{mag}$	$f(\lambda)/f(\lambda_0)$
0.3382	2.957	1.101	0.602	0.574
0.3392	2.948	1.099	0.607	0.572
0.3441	2.906	1.092	0.631	0.559
0.3504	2.854	1.081	0.659	0.545
0.3567	2.803	1.067	0.684	0.533
0.3634	2.752	1.050	0.708	0.521
0.3648	2.741	1.046	0.712	0.519
0.3703	2.701	1.028	0.726	0.512
0.3774	2.650	0.588	0.328	0.739
0.3846	2.600	0.070	-0.149	1.147
0.3860	2.591	0.028	-0.184	1.185
0.3906	2.560	-0.027	-0.213	1.217
0.4032	2.480	-0.033	-0.150	1.148
0.4040	2.475	-0.032	-0.145	1.143
0.4082	2.450	-0.029	-0.119	1.116
0.4167	2.400	-0.016	-0.061	1.058
0.4190	2.387	-0.012	-0.046	1.043
0.4255	2.350	0.000	0.000	1.000
0.4367	2.290	0.019	0.075	0.933
0.4464	2.240	0.037	0.141	0.878
0.4566	2.190	0.054	0.207	0.826
0.4590	2.179	0.057	0.221	0.816
0.4673	2.140	0.072	0.275	0.776
0.4785	2.090	0.091	0.346	0.727
0.4902	2.040	0.110	0.417	0.681
0.5000	2.000	0.126	0.476	0.645
0.5060	1.976	0.135	0.511	0.625
0.5127	1.950	0.147	0.552	0.601
0.5261	1.901	0.167	0.628	0.561
0.5550	1.802	0.213	0.790	0.483
0.5554	1.800	0.214	0.793	0.482
0.5798	1.725	0.251	0.923	0.427
0.5868	1.704	0.262	0.960	0.413
0.6033	1.658	0.288	1.046	0.382

From the solutions to the system of linear equations derived for the network of stars, an estimate of the internal consistency of the original photometry can be made. For a given wavelength, the spectrophotometric gradients are computed from Table 4 and compared with the actual observed values. An error-distribution curve

Table 4. Smoothed relative SED

Star	$\epsilon$ Ori	$\beta$ Cen	$\alpha$ Vir	$\alpha$ Cru	$\alpha$ Pav	$\alpha$ Eri	$\alpha$ Gru	$\alpha$ Leo	$\beta$ Ori	$\epsilon$ Sgr	$\alpha$ CMa	$\alpha$ Car
Spectral type	B0 Ia	B1 II	B1 V	B2	B3 IV	B5 V	B5 V	B7 V	B8 Ia	B9 IV	A1 V	F0 Ia
V	1.70	0.63	0.9v	0.85	1.95	0.51	1.76	1.36	0.14v	1.81	-1.42	-0.72
$\lambda(\mu)$	$f(\lambda)/f(0.4255)$											
0.3392	2.006	1.842	1.754	1.886	1.368	1.162	0.966	0.737	1.189	0.466	0.516	0.284
0.3441	1.920	1.759	1.689	1.798	1.319	1.125	0.941	0.725	1.157	0.466	0.512	0.288
0.3504	1.815	1.657	1.597	1.692	1.264	1.080	0.910	0.718	1.124	0.466	0.507	0.293
0.3567	1.712	1.562	1.512	1.591	1.209	1.038	0.881	0.701	1.104	0.466	0.502	0.298
0.3634	1.611	1.470	1.424	1.486	1.153	0.997	0.850	0.684	1.098	0.465	0.495	0.312
0.3703	1.516	1.382	1.346	1.391	1.106	0.975	0.829	0.674	1.126	0.506	0.498	0.446
0.3846	1.396	1.366	1.397	1.407	1.339	1.343	1.217	1.212	1.283	1.196	1.056	1.097
0.3860	1.414	1.411	1.407	1.431	1.383	1.353	1.278	1.267	1.299	1.236	1.134	1.131
0.3906	1.361	1.375	1.374	1.392	1.354	1.330	1.306	1.278	1.268	1.246	1.214	1.157
0.4032	1.195	1.211	1.207	1.211	1.217	1.195	1.184	1.167	1.156	1.151	1.149	1.105
0.4082	1.144	1.159	1.155	1.159	1.170	1.145	1.138	1.127	1.117	1.114	1.113	1.079
0.4167	1.069	1.075	1.073	1.073	1.094	1.072	1.067	1.062	1.055	1.057	1.055	1.038
0.4255	1.000	1.000	1.000	1.000	1.000	1.000	1.000	1.000	1.000	1.000	1.000	1.000
0.4367	0.924	0.920	0.920	0.918	0.944	0.925	0.925	0.927	0.938	0.934	0.934	0.953
0.4464	0.865	0.856	0.856	0.854	0.881	0.865	0.865	0.912	0.889	0.881	0.883	0.918
0.4566	0.810	0.794	0.797	0.793	0.820	0.808	0.809	0.816	0.842	0.833	0.832	0.880
0.4673	0.758	0.738	0.741	0.737	0.763	0.756	0.756	0.779	0.797	0.785	0.783	0.846
0.5000	0.622	0.594	0.598	0.589	0.618	0.628	0.619	0.629	0.680	0.659	0.658	0.751
0.5127	0.578	0.549	0.551	0.542	0.571	0.588	0.574	0.585	0.641	0.617	0.617	0.716
0.5261	0.535	0.506	0.507	0.498	0.527	0.551	0.531	0.544	0.603	0.578	0.578	0.683
0.5556	0.454	0.427	0.422	0.414	0.443	0.482	0.451	0.464	0.529	0.503	0.505	0.617
0.5868	0.384	0.360	0.347	0.344	0.371	0.422	0.380	0.395	0.461	0.438	0.443	0.555

results which is fairly well-determined, because we have a sample population of 100. Assuming a Gaussian distribution for these error curves, we may define the error introduced by the observational photometry and the reduction process to be proportional to the standard deviation of the error distribution at each wavelength. A typical error distribution is shown in Fig. 9, where the number of comparisons is plotted vs the magnitude difference between the computed and observed spectro-photometric gradients. The variation with wavelength of the standard deviations of these error distributions is shown in Fig. 10. Upon examining this Figure, it should be borne in mind that the observed brightness of a star vanishes at short wavelengths because of atmospheric extinction, and vanishes at long wavelengths because of

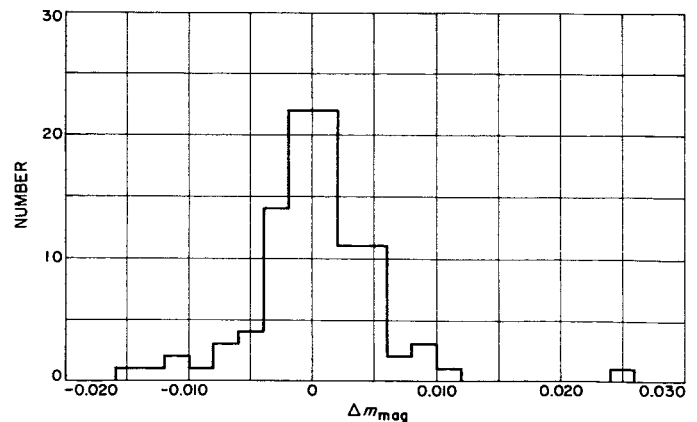


Fig. 9. Distribution of errors for  
 $\lambda = 0.437 \mu$



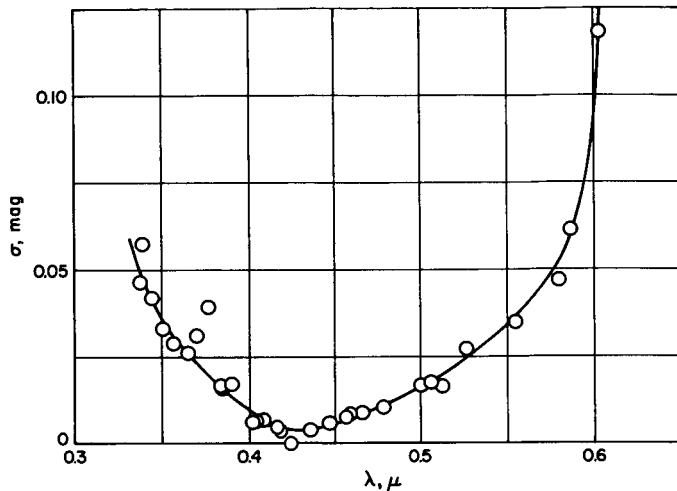


Fig. 10. Variation with wavelength of the standard deviation of a single observation

the sensitivity curve of the photomultiplier tube. This explains the large standard deviations at the ends of the mean curve in Fig. 10, and indicates that the photometry, and hence the derived stellar energy distributions, are uncertain outside the wavelength range 0.37–0.54  $\mu$ . For small magnitude differences, the relation

$$\pm 0.01 \text{ mag} = \pm 1\%$$

may be used to judge the accuracy of the photometry, as presented in Fig. 10.

It should also be emphasized that this standard deviation is the standard deviation of a single observation, and would be the uncertainty in the derived stellar energy distributions if there were exactly one observation per unknown. In actual fact, the redundancy of the least-squares solution is four to one, so that a good approximation is to divide the standard deviations of Fig. 10 by  $(4)^{1/2}$ ; these would then represent the expected standard deviations for the stellar energy distributions presented in this Report. We thus conclude that the random (rms) uncertainties of the results in Table 4 are

$$\begin{aligned} 0.36 \leq \lambda \leq 0.56 & \pm 1\% \\ \lambda < 0.36 & \pm 2\% \\ \lambda > 0.56 & \pm 5\% \end{aligned}$$

A fundamental point must now be emphasized. The SED of every star in our network of stars depends upon the SED assumed for the standard star. In our case, we have to adopt an intermediate star as a standard because Vega is not observable in the Southern Hemisphere. Thus, an additional uncertainty is introduced over and above the uncertainties in the observations just discussed. Even more important, any systematic error present in the intermediate standard star will be reflected directly in the SED of all our stars.

As seen from Fig. 4, which shows an actual scanner tracing, the true SED lies below the curve adopted to represent the continuum. We must therefore correct the SED given in Table 4 for the effect of the absorption lines. A simple method of doing this is to measure two

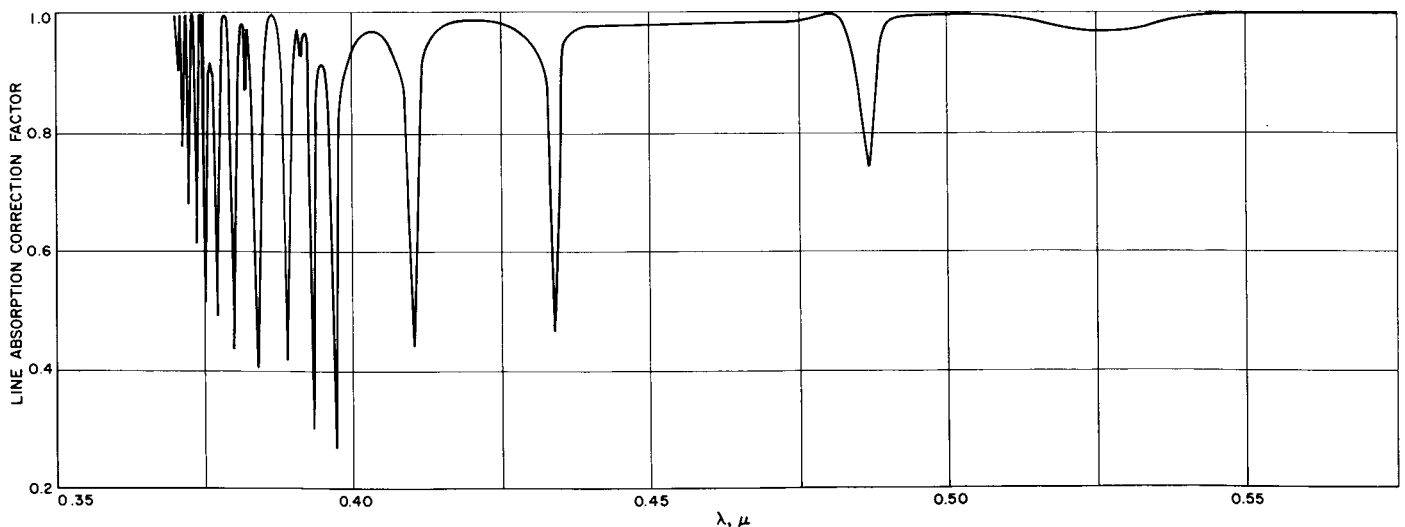


Fig. 11. Line-absorption correction factor for Canopus

deflections at each wavelength on the original scanner tracing. The first is the deflection to the continuum,  $d_{cont}$ ; the second is the deflection to the true SED,  $d_{true}$ . Take the ratio  $d_{true}/d_{cont}$  for a given star as a function of wavelength and multiply the relative SED given for this star in Table 4. This line-absorption correction factor is shown in Fig. 11 for Canopus. It is evident that the correction is greatest in the region of the peak of the SED. The continuum derived for Canopus in Table 4 was multiplied by the correction curve shown in Fig. 11 and averaged over 100-Å intervals. This smoothed SED, normalized to unity at its peak, is given in Table 5 and shown in Fig. 12. Also shown in Fig. 12, as a dotted line, is the uncorrected SED of Canopus given in Table 4. The correction for absorption lines has not been com-

puted for the eleven remaining stars in Table 4, but reproductions of actual scanner tracings of these stars are contained in Appendix B, from which the correction may be estimated.

**Table 5. Relative SED of Canopus<sup>a</sup>**

$\lambda$ , $\mu$	$f(\lambda)/f_{peak}$	$\lambda$ , $\mu$	$f(\lambda)/f_{peak}$
0.340	0.289	0.455	0.876
0.350	0.296	0.460	0.864
0.360	0.307	0.465	0.856
0.370	0.393	0.470	0.839
0.375	0.539	0.475	0.818
0.380	0.690	0.480	0.787
0.385	0.897	0.485	0.713
0.390	0.960	0.490	0.722
0.395	0.935	0.495	0.763
0.400	0.914	0.500	0.761
0.405	0.993	0.510	0.735
0.410	0.945	0.520	0.709
0.415	0.959	0.530	0.682
0.420	1.000	0.540	0.660
0.425	0.985	0.550	0.638
0.430	0.882	0.560	0.617
0.435	0.850	0.570	0.597
0.440	0.917	0.580	0.577
0.445	0.904	0.590	0.558
0.450	0.888	0.600	0.539

<sup>a</sup> Corrected for absorption lines, averaged over 100-Å intervals, and normalized to unity at the peak.

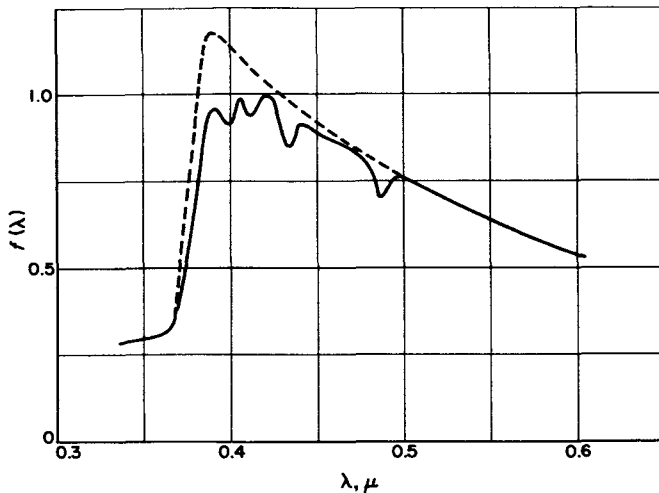


**Fig. 12. Relative SED of Canopus corrected for absorption lines**

## V. CALIBRATION TO ABSOLUTE UNITS

The SED thus far discussed have been relative in the sense that only a constant factor is required to have the absolute SED in units of  $w/cm^2/\mu$  outside the Earth's atmosphere. This section will discuss one method by which this constant factor may be determined.

The monochromatic fluxes of the Sun have been measured by Minnaert (Ref. 9), and the apparent visual magnitude  $V$ , on the Johnson  $UBV$  system, has been measured by Stebbins and Kron (Ref. 10). From these, we can compute that the monochromatic flux incident

outside the Earth's atmosphere from a G2 V star (same spectral type as the Sun) of apparent visual magnitude  $V = 0.00$  is  $3.79 \times 10^{-12} \text{ w/cm}^2/\mu$  at  $\lambda = 0.5465 \mu$ . The absolute monochromatic fluxes of stars were also measured by Willstrop (Ref. 6), who gives a value of  $3.8 \times 10^{-12} \text{ w/cm}^2/\mu$  at  $\lambda = 0.570 \mu$  for a star of visual magnitude  $V = 0.00$  and color index  $B - V = 0.00$  outside the Earth's atmosphere. Code (Ref. 3), in his investigation of stellar energy distributions, obtained a value of  $3.9 \times 10^{-12} \text{ w/cm}^2/\mu$  at  $\lambda = 0.556 \mu$ . For our purposes, we assume, for a star with apparent visual magnitude  $V = 0.00$  and color index  $B - V = 0.00$ , a value of  $3.8 \times 10^{-12} \text{ w/cm}^2/\mu$  for the monochromatic flux outside the Earth's atmosphere at  $\lambda = 0.556 \mu$  to calibrate our relative SED.

The simplest procedure is to scale this calibration factor using the star's apparent visual magnitude

$$f_{0.556}(V) = f_{0.556}(V = 0.00) 10^{-0.4 V} \quad (24)$$

$$= 3.8 \times 10^{-12} \times 10^{-0.4 V} \quad (25)$$

The published apparent visual magnitude  $V$  for Canopus (Ref. 11) is  $V = -0.72$  magnitudes. Thus

$$f_{0.556}(-0.72) = 7.4 \times 10^{-12} \text{ w/cm}^2/\mu \quad (26)$$

From Table 5, the peak value of Canopus is then

$$f_{\text{peak}} = 1.18 \times 10^{-11} \text{ w/cm}^2/\mu \quad (27)$$

A more accurate determination of the normalization constant is to recognize that for stars of earlier types than Canopus (for example, Vega), the peak of the SED falls at a shorter wavelength. Thus, the contribution to the visual-magnitude bandpass is different, and the simple scaling procedure is not exact. If we obtain a set of *UBV* sensitivity curves, integrate with them the relative SED (including absorption lines), and express the results in terms of the *observed UBV* magnitudes, the normalization constant can be determined for any star.

The *UBV* sensitivity curves are taken from Arp (Ref. 12) and are reproduced in Table 6. The definition of the apparent visual magnitude  $V$  on this system is

$$V = -2.5 \log_{10} \int_0^{\infty} f(\lambda) V(\lambda) d\lambda + C \quad (28)$$

Table 6. The Johnson *UBV* bandpasses

$\lambda, \mu$	$U(\lambda)$	$B(\lambda)$	$V(\lambda)$
	arbitrary units		
0.2941	0.000	—	—
0.3030	0.066	—	—
0.3125	0.346	—	—
0.3226	0.777	—	—
0.3333	1.300	—	—
0.3448	1.813	—	—
0.3571	2.178	0.000	—
0.3704	2.330	0.075	—
0.3846	1.426	0.640	—
0.4000	0.197	2.523	—
0.4167	0.000	2.915	—
0.4348	—	3.006	—
0.4545	—	2.683	—
0.4762	—	2.015	0.000
0.4878	—	1.64	0.112
0.5000	—	1.286	0.993
0.5128	—	0.91	2.104
0.5263	—	0.505	2.789
0.5405	—	0.20	2.808
0.5556	—	0.000	2.486
0.5714	—	—	1.990
0.5882	—	—	1.518
0.6060	—	—	0.930
0.6250	—	—	0.473
0.6452	—	—	0.183
0.6667	—	—	0.099
0.6897	—	—	0.049
0.7143	—	—	0.021
0.7407	—	—	0.000

where  $V(\lambda)$  is the Johnson *V* bandpass presented in Table 6, and  $f(\lambda)$  is the true SED in physical units, which we wish to determine. Equation 28 can be rewritten

$$f'(\lambda) = \frac{f(\lambda)}{f_{\text{peak}}} \quad (29)$$

and then

$$V = -2.5 \log_{10} \int_0^{\infty} f'(\lambda) V(\lambda) d\lambda - 2.5 \log_{10} f_{\text{peak}} + C \quad (30)$$

where  $f'(\lambda)$  is now the relative SED of the star, including absorption lines and normalized to unity at the peak.

Table 7. *UBV* magnitudes of Vega and Canopus

Star	<i>U</i>	<i>B</i>	<i>V</i>
Vega	+0.03	+0.04	+0.04
Canopus	-0.52	-0.56	-0.72

Vega has a visual magnitude  $V = +0.04$  and a color index  $B - V = 0.00$  mag (Ref. 11). Thus, we expect the monochromatic flux at  $0.5560 \mu$  to be

$$f(0.5560)_{\text{vega}} = 3.66 \times 10^{-12} \text{ w/cm}^2/\mu \quad (31)$$

and from the SED given by Code (Ref. 3), we have

$$f_{\text{peak,vega}} = 6.16 \times 10^{-12} \text{ w/cm}^2/\mu \quad (32)$$

The observed *UBV* magnitudes of Vega and Canopus (Ref. 11) are given in Table 7.

By numerically evaluating the integrals appearing in Eq. 30 and inserting the *V* magnitude and  $f_{\text{peak}}$  value for Vega, we determine the constant *C*. The result is

$$C = -29.99 \quad (33)$$

We now invert the process, re-evaluating the integral in Eq. 3, using the relative SED corrected for absorption

Table 8. Parameters of model atmosphere for Canopus

Effective temperature	7,000°K
Surface gravity	100 cm sec <sup>-2</sup>

lines, and the observed *V* magnitude of Canopus, together with the computed value of *C* to obtain the peak monochromatic flux of Canopus. In order to perform the integrations, the available relative SED of Canopus needs to be extended. A model stellar atmosphere (Ref. 13) was computed for Canopus and used to extend the continuum to the infrared. The parameters used for this model atmosphere are contained in Table 8.

Figure 13 shows the predicted SED of the model atmosphere, the uncorrected SED of Canopus given in Table 4, and the energy distribution of Canopus corrected for absorption lines.

As the final result, we obtain the peak monochromatic flux of Canopus

$$f_{\text{peak}} = 1.22 \times 10^{-11} \text{ w/cm}^2/\mu$$

at

$$\lambda = 0.420 \mu.$$

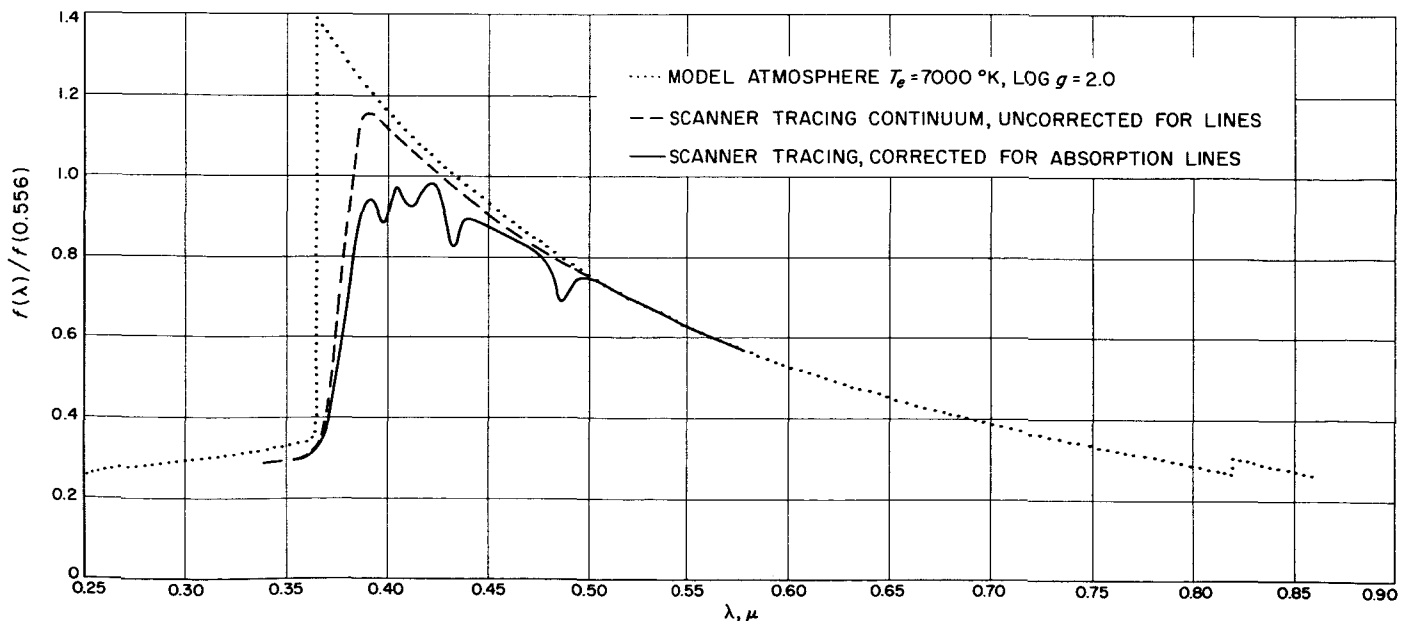


Fig. 13. SED of Canopus

## VI. FUTURE PLANS

The computer program as it is written uses spectrophotometric gradients, which are in reality intensity ratios of two stars, as the input data in setting up the network equations. Thus, the system really becomes independent of the observatory, telescope, etc. It would be feasible to enlarge the network of stars to 40 or so, covering the entire celestial sphere and including Vega. In this manner, some of the present uncertainties in the absolute SED of the southern stars, including Canopus, could be removed.

By far, the most improvement would come from a better determination of the absolute SED of Vega. As Section III indicates, almost all of the uncertainties in the energy distribution of Canopus comes from this source. The present uncertainties (rms) in the SED of Vega have been estimated by Oke to be

$$\lambda < 0.37\mu \pm 5\%$$

$$\lambda > 0.37\mu \pm 1\%$$

## NOMENCLATURE

$a, b$	constants in modified Rayleigh law for atmospheric extinction
$d$	measured scanner deflection, in arbitrary units
$f$	SED, in flux units
$\mathcal{G}$	amplifier gain, in magnitudes
$g, G$	spectrophotometric gradient, in magnitudes
$h$	hour angle, in radians
$k$	extinction coefficient, in magnitudes per air mass
$m, M$	monochromatic magnitudes
$s$	index on spectrophotometric gradient
$t$	sidereal time, in hours
$U, B, V$	apparent magnitudes in $UBV$ system, outside the Earth's atmosphere
$U(\lambda), B(\lambda), V(\lambda)$	spectral bandpasses of the $UBV$ system
$X$	air mass
$w, W$	weights
$z$	zenith angle
$\alpha$	right ascension, in hours
$\delta$	declination, in radians
$\lambda$	wavelength, in microns
$\phi$	latitude, in radians

## REFERENCES

1. Scull, J. R., *The Application of Optical Sensors for Lunar and Planetary Space Vehicles*, Technical Report No. 32-274, Jet Propulsion Laboratory, Pasadena, California, May 31, 1962.
2. Johnson, H. L., and Morgan, W. W., "Fundamental Stellar Photometry for Standards of Spectral Type on the Revised System of the Yerkes Spectral Atlas," *Astrophysical Journal*, Vol. 117, p. 313, May 1953.
3. Code, A. D., "Stellar Energy Distributions," *Stellar Atmospheres*, ed. by J. L. Greenstein, University of Chicago Press, Chicago, Illinois, 1960, chapter 2, p. 50.
4. Oke, J. B., "Standard Stars for Photoelectric Spectrophotometry," *Astrophysical Journal*, Vol. 131, p. 358, March 1960.
5. Woolley, R. v. d. R., Gascoigne, S. C. B., and de Vaucouleurs, A., "Photographic Observations of Monochromatic Magnitude at Six Wavelengths," *Monthly Notices of the Royal Astronomical Society*, Vol. 114, p. 490, 1954.
6. Willstrop, R. V., "Absolute Measures of Stellar Radiation," *Monthly Notices of the Royal Astronomical Society*, Vol. 121, p. 120, 1960.
7. Hardie, R. H., "Photoelectric Reductions," *Astronomical Techniques*, ed. by W. A. Hiltner, University of Chicago Press, Chicago, Illinois, 1962, chapter 8, p. 178.
8. Cohen, E. R., Crowe, K. M., and Dumond, J. W., *The Fundamental Constants of Physics*, Interscience Publishers, New York, 1957.
9. Minnaert, M., "The Photosphere," *The Sun*, ed. by G. P. Kuiper, University of Chicago Press, Chicago, Illinois, 1956, chapter 3, p. 88.
10. Stebbins, J., and Kron, G. E., "Six-Color Photometry of Stars. X. The Stellar Magnitude and Color Index of the Sun," *Astrophysical Journal*, Vol. 126, p. 266, September 1957.
11. *The Observer's Handbook*, Royal Astronomical Society of Canada, Toronto, Ontario, 1963, p. 70.
12. Arp, H., *Astrophysical Journal*, Vol. 133, page 874, May 1961.
13. Norton, R. H., *HeH<sup>+</sup> in Model Stellar Atmospheres*, doctoral thesis, California Institute of Technology, Pasadena, California, May 1964.

## APPENDIX A

## Computational Procedures and Network Reduction Equations

The basic notation is as follows:

$M_i$	=	true relative monochromatic magnitude of star $i$
$m_i$	=	observed relative monochromatic magnitude of star $i$
$G_{ij}$	=	true spectrophotometric gradient between stars $i$ and $j$
$g_{ij}$	=	observed spectrophotometric gradient between stars $i$ and $j$
$s = s(i, j)$	=	matrix assigning an index to a given pair $i, j$ of stars observed on the same night. When the same pair of stars is again observed on another night, from this matrix the combination is given the same index. On each and every night, the stars observed are ordered in increasing right ascension to ensure that all gradients are computed in the same sense.

We thus have

$$\left. \begin{aligned} G_{ij} &= M_i - M_j = G_s \\ g_{ij} &= m_i - m_j = g_s \end{aligned} \right\} i > j \quad (\text{A-1})$$

$$(\text{A-2})$$

Let

$n$	=	index on night
$j$	=	index of any star on a given night
$k$	=	index on scanner tracing of this star
$K$	=	number of traces taken on this star
$\lambda$	=	wavelength in microns
$d_{jk}(\lambda)$	=	measured scanner deflection (arbitrary units)
$\mathcal{G}_{jk}(\lambda)$	=	amplifier gain in magnitudes
$t_{jk}(\lambda)$	=	sidereal time in hours
$z_{jk}(\lambda)$	=	zenith angle of star in radians
$w_{jk}(\lambda)$	=	assigned weight of this observation

$k(\lambda)$	=	extinction coefficient in magnitudes
$\phi$	=	latitude of observatory in radians
$\alpha_j$	=	right ascension of star in hours
$\delta_j$	=	declination of star in radians
$w_{jk}(\lambda)$	=	$\begin{cases} 0 & \text{if no observation or if bad observation} \\ 1 & \text{if result of trace in single direction} \\ 2 & \text{if mean of forward and reverse traces} \end{cases}$

The computational procedure is as follows:

Compute hour angle

$$h_{jk}(\lambda) = \pi \left[ \frac{t_{jk}(\lambda) - \alpha_j}{12} \right] \quad (\text{A-3})$$

Compute secant of zenith angle

$$[\sec z_{jk}(\lambda)]^{-1} = \cos \phi \cos h_{jk}(\lambda) \cos \delta_j + \sin \phi \sin \delta_j \quad (\text{A-4})$$

Correct the scanner deflection for the amplifier gain and atmospheric extinction

$$r = k(\lambda) \sec z_{jk}(\lambda) - \mathcal{G}_{jk}(\lambda) \quad (\text{A-5})$$

$$f'_{jk}(\lambda) = d_{jk}(\lambda) 10^{-0.4 r} \quad (\text{A-6})$$

Each trace is normalized relative to an arbitrary zero-point wavelength

$$f_{jk}(\lambda) = \frac{f'_{jk}(\lambda)}{f'_{jk}(\lambda_0)} \quad (\text{A-7})$$

Now, take the weighted mean of all traces on this star on this night

$$w'_j(\lambda) = \sum_{k=1}^K w_{jk}(\lambda) \quad (\text{A-8})$$

$$\overline{f_j(\lambda)} = \frac{1}{w'_j(\lambda)} \sum_{k=1}^K w_{jk}(\lambda) f_{jk}(\lambda) \quad (\text{A-9})$$

Then

$$m_j(\lambda) = -2.5 \log_{10} \overline{f_j(\lambda)} \quad (\text{A-10})$$

Form all possible gradients between stars observed on this night and assign an index to indicate the night

$$g_{sn}(\lambda) = m_i(\lambda) - m_j(\lambda) \quad (\text{A-11})$$

$$i > j$$

This gradient is assigned the weight

$$w_{sn}(\lambda) = w'_i(\lambda) w'_j(\lambda) \quad (\text{A-12})$$

Now, form the weighted mean gradients over all nights

$$W_s(\lambda) = \sum_{n=1}^N w_{sn}(\lambda) \quad (\text{A-13})$$

$$T = \frac{1}{W_s(\lambda)} \sum_{n=1}^N w_{sn}(\lambda) 10^{-0.4 g_{sn}(\lambda)} \quad (\text{A-14})$$

$$\overline{g_s(\lambda)} = -2.5 \log_{10} T \quad (\text{A-15})$$

In the present program,  $N = 30$ ,  $s = 1, 2, 3 \dots s_{max}$ ,  $s_{max} = 100$ . Now, write generalized expressions for Eq. A-1 and A-2

$$G_s = \sum_{k=1}^n x_{ks} M_k \quad (\text{A-16})$$

$$g_s = \sum_{k=1}^n x_{ks} m_k \quad (\text{A-17})$$

where

$$x_{ks} = x_{k,i,j} = \begin{cases} +1 & \text{if } k = i \\ 0 & \text{if } k \neq i \text{ or } j \\ -1 & \text{if } k = j \end{cases} \quad (\text{A-18})$$

and  $n$  = number of stars on list ( $n = 25$  in the present program). The least-squares criterion is

$$\sum_{s=1}^{s_{max}} W_s [G_s - g_s]^2 = \text{minimum} \quad (\text{A-19})$$

where  $s_{max}$  = total number of gradients in network.

Insert Eq. A-17 into A-19

$$\sum_{s=1}^{s_{max}} W_s \left[ \sum_{k=1}^n x_{ks} M_k - g_s \right]^2 = \text{minimum} \quad (\text{A-20})$$

Differentiate Eq. A-20 with respect to each of the  $M_k$  in turn and equate to zero, reversing the order of summation

$$\sum_{k=1}^n \left[ \sum_{s=1}^{s_{max}} W_s x_{is} x_{ks} \right] M_k = \sum_{s=1}^{s_{max}} x_{is} W_s g_s$$

$$i = 1, 2, 3 \dots n \quad (\text{A-21})$$

We thus have the system of linear equations

$$\sum_{k=1}^n C_{ik} M_k = d_i$$

$$i = 1, 2 \dots n \quad (\text{A-22})$$

where

$$C_{ik} = \sum_{s=1}^{s_{max}} x_{is} x_{ks} W_s \quad (\text{A-23})$$

$$d_i = \sum_{s=1}^{s_{max}} x_{is} W_s g_s \quad (\text{A-24})$$

These equations as they stand are not linearly independent. We thus replace the  $q^{\text{th}}$  equation by

$$M_q = M(\lambda)$$

where

$q$  = index of star selected as standard star

$M(\lambda)$  = adopted monochromatic magnitude of standard star



For each wavelength in turn, a system of equations is set up and solved, as described above. In the present program, 34 sets of 25 equations each must be solved to determine the best SED to fit the available data.

Formerly, reduction procedures have determined the SED of the stars in a stepwise fashion, starting from the standard star and proceeding around the celestial sphere, hoping that there would be no closing error and

that the original energy distribution of the standard star would be obtained when the celestial sphere had been circumnavigated. In general, a closing error is present, and adjustments (of an arbitrary nature) must be made. It is to be emphasized that the present procedure, based upon the condition of minimum error, ensures that no closing error exists and that the energy distribution of every star in the network is consistent with the entire network.

## APPENDIX B

## Reproductions of Actual Scanner Tracings

The spectral-energy distribution (SED) of 11 of the 12 stars discussed in this Report are presented in actual scanner tracings (Figs. B-1 through B-11).<sup>3</sup> In all cases, the horizontal scale is *wavelength*, increasing to the left, and the vertical scale is *observed intensity*, in arbitrary units. The scales are not the same for all stars. The Bayer designation and star name are given for each star.

<sup>3</sup>A tracing for  $\alpha$  Vir is not available.

These reproductions are included in order to be able to estimate the effect of stellar absorption lines. The true SED correspond to the lower curves, containing the absorption lines, while the SED presented in Table 4 correspond to the upper curves, which are more or less envelopes to the true SED. To obtain the true SED of a particular star, follow the procedure outlined for Canopus, taking the ratio between the two curves given for the star and multiplying the SED given for the star in Table 4 by this ratio.

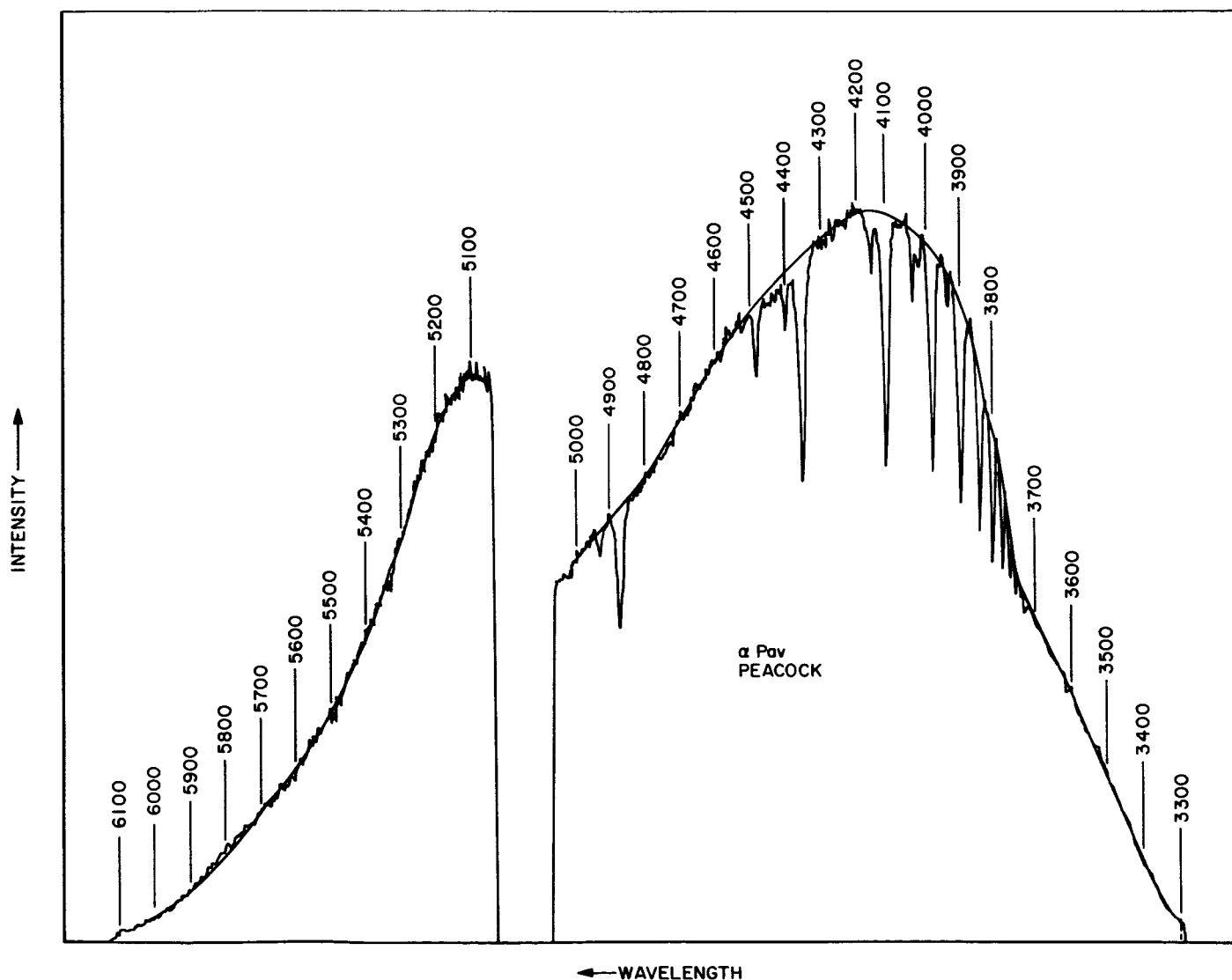


Fig. B-1. Reproduction of actual scanner tracing

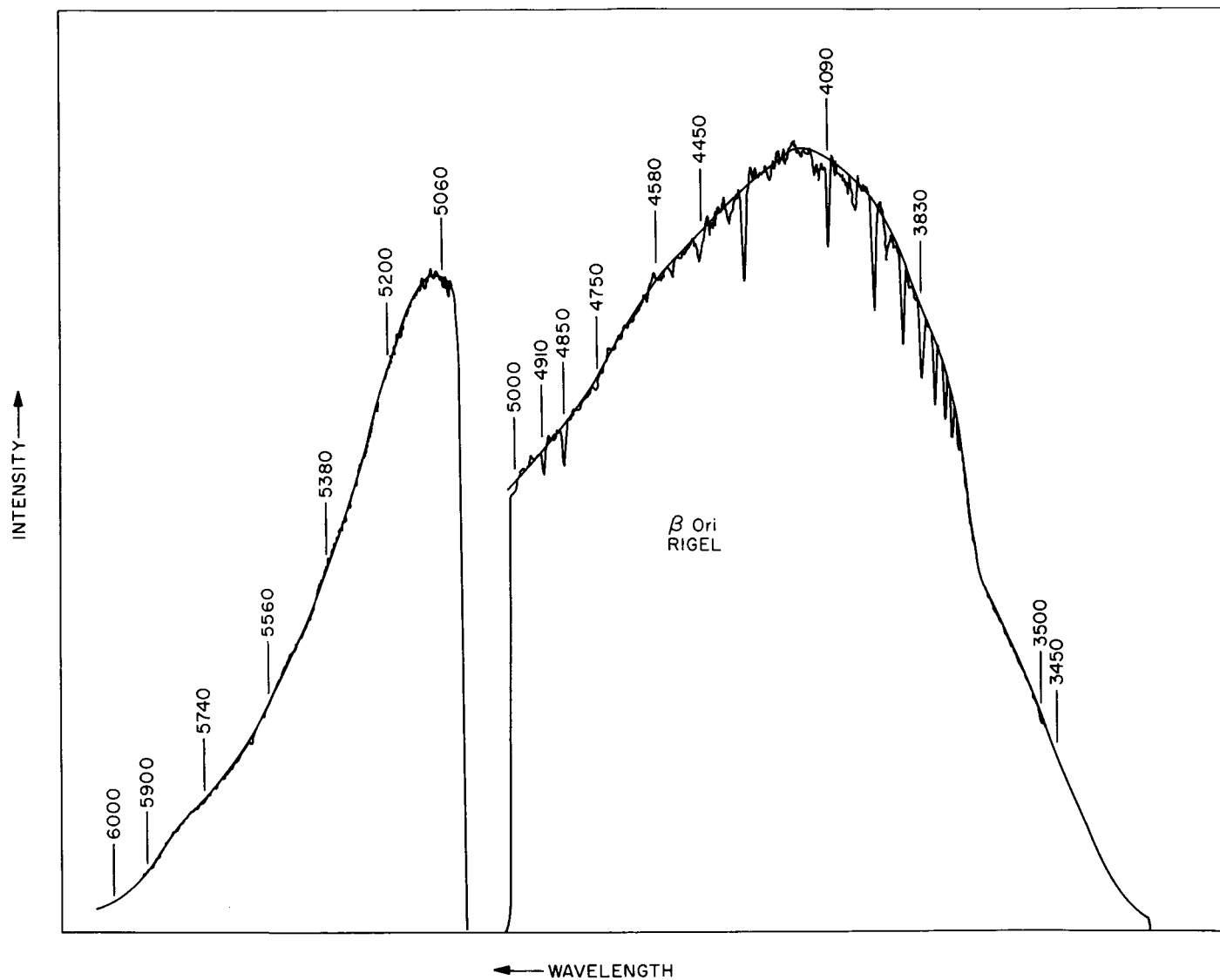


Fig. B-2. Reproduction of actual scanner tracing

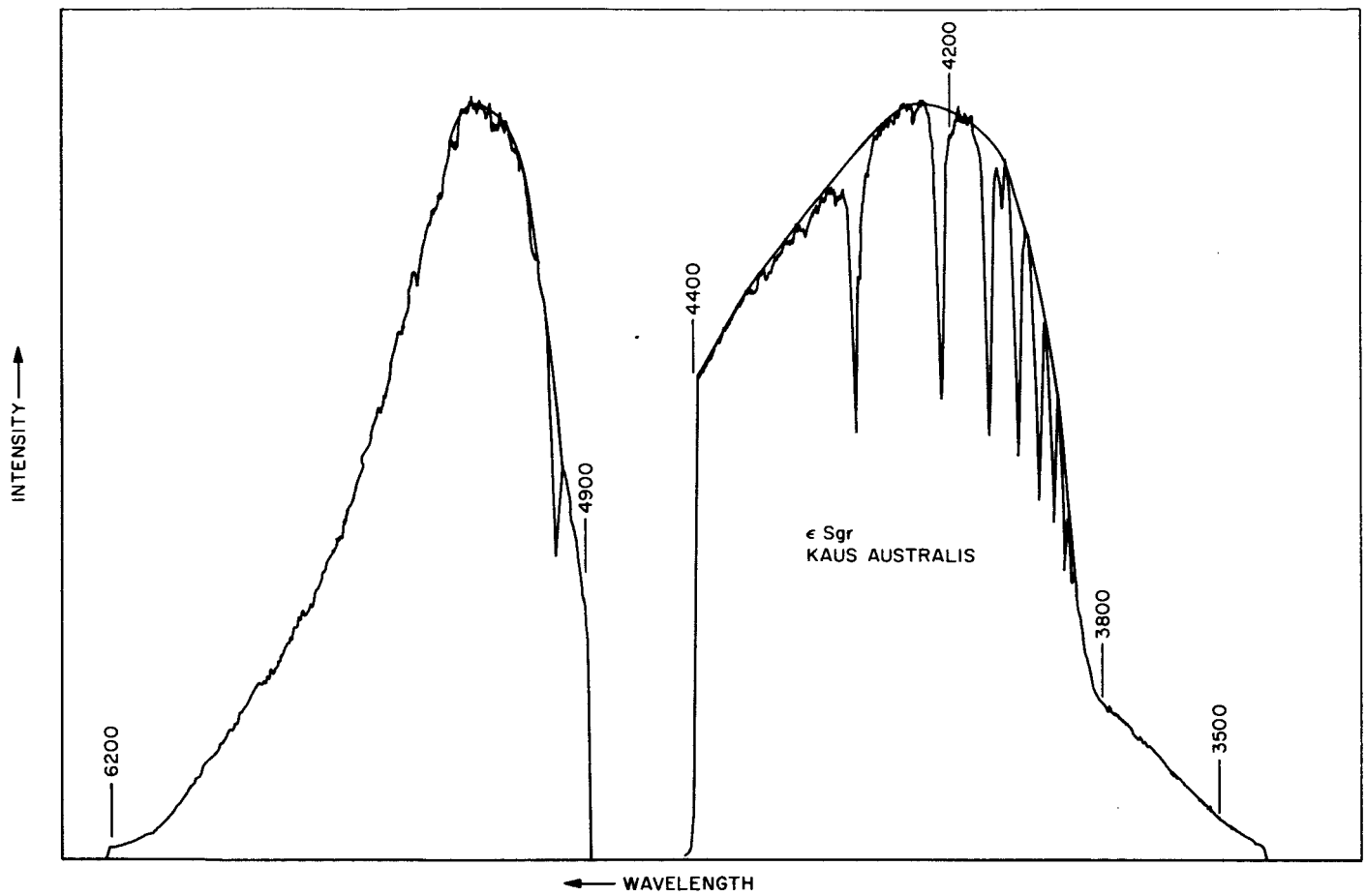


Fig. B-3. Reproduction of actual scanner tracing

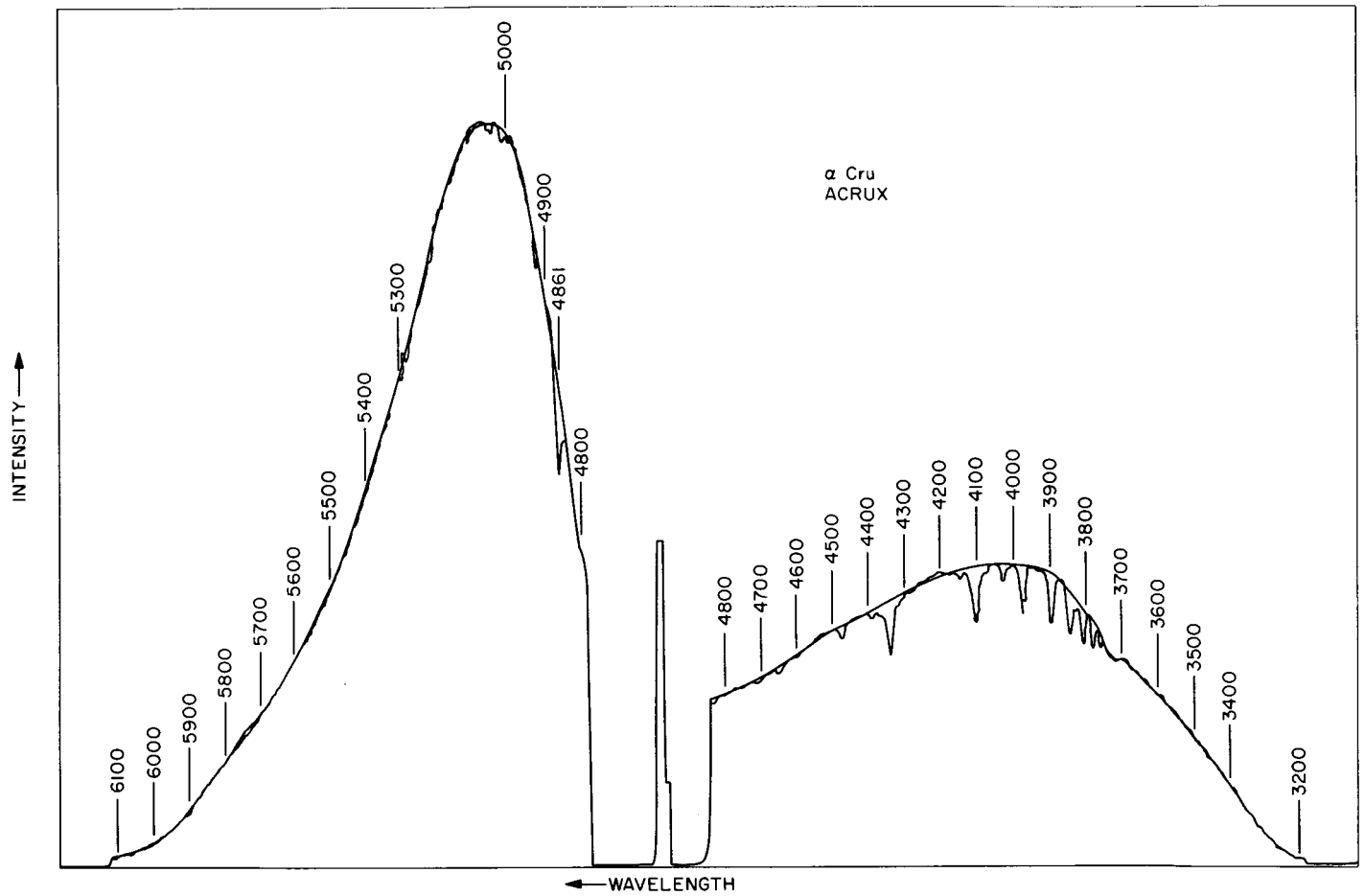


Fig. B-4. Reproduction of actual scanner tracing

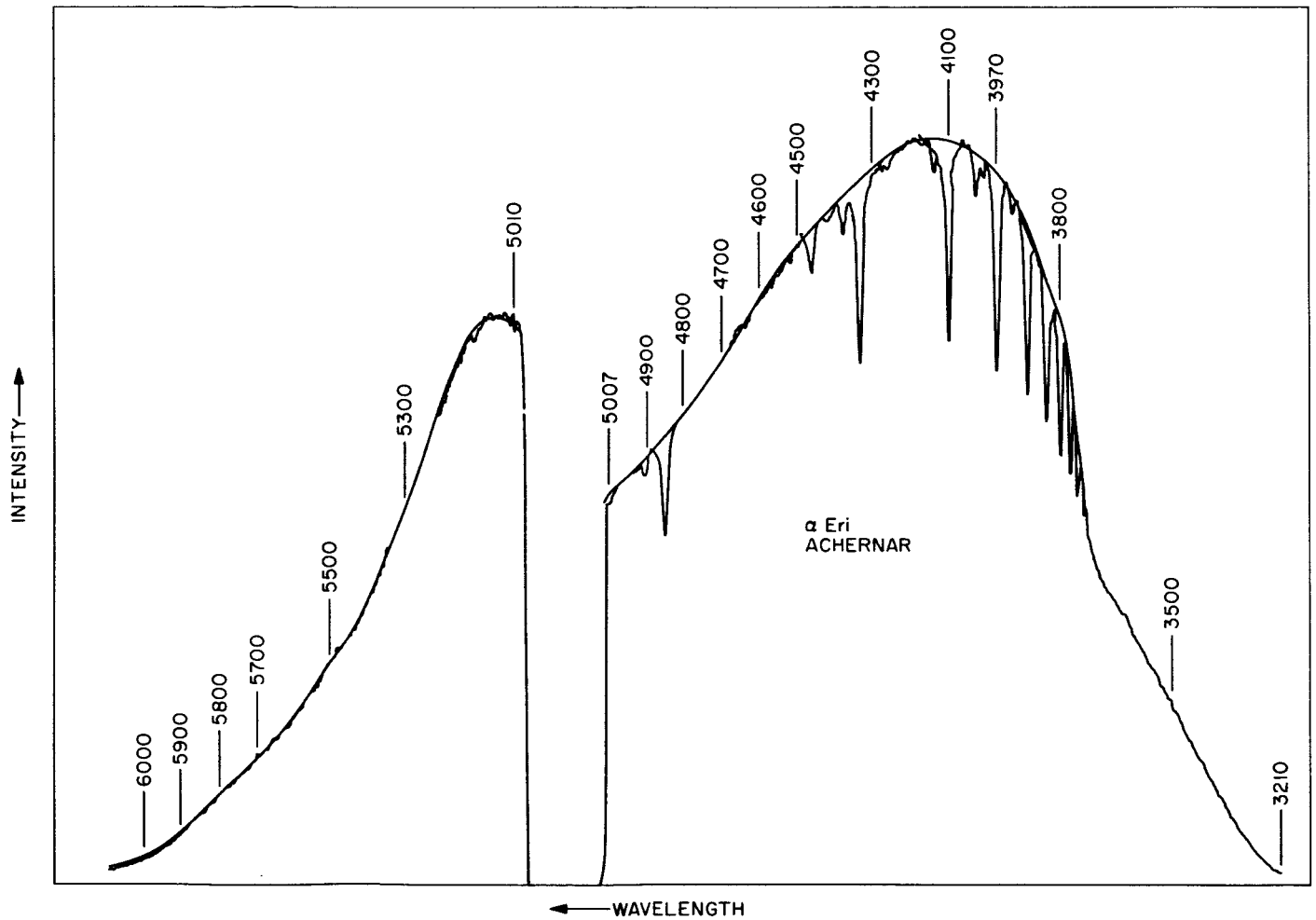


Fig. B-5. Reproduction of actual scanner tracing

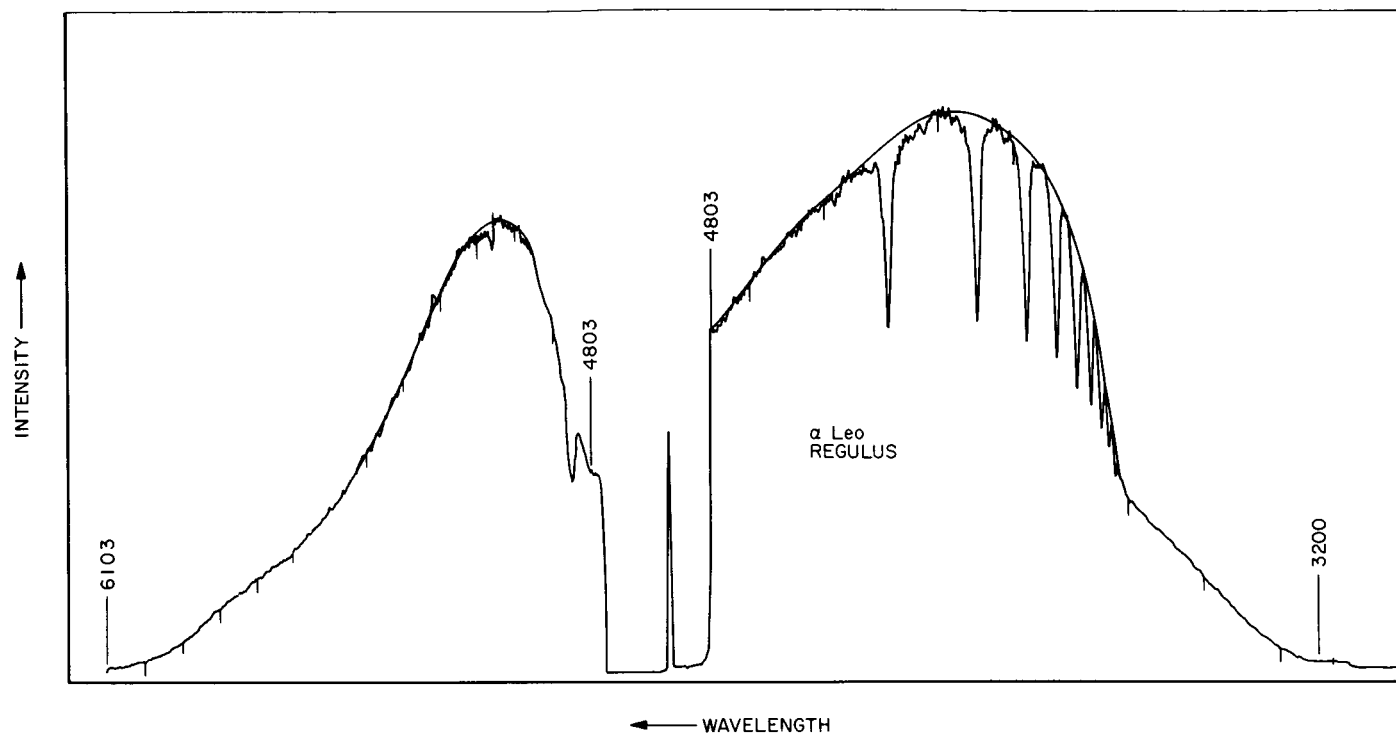


Fig. B-6. Reproduction of actual scanner tracing

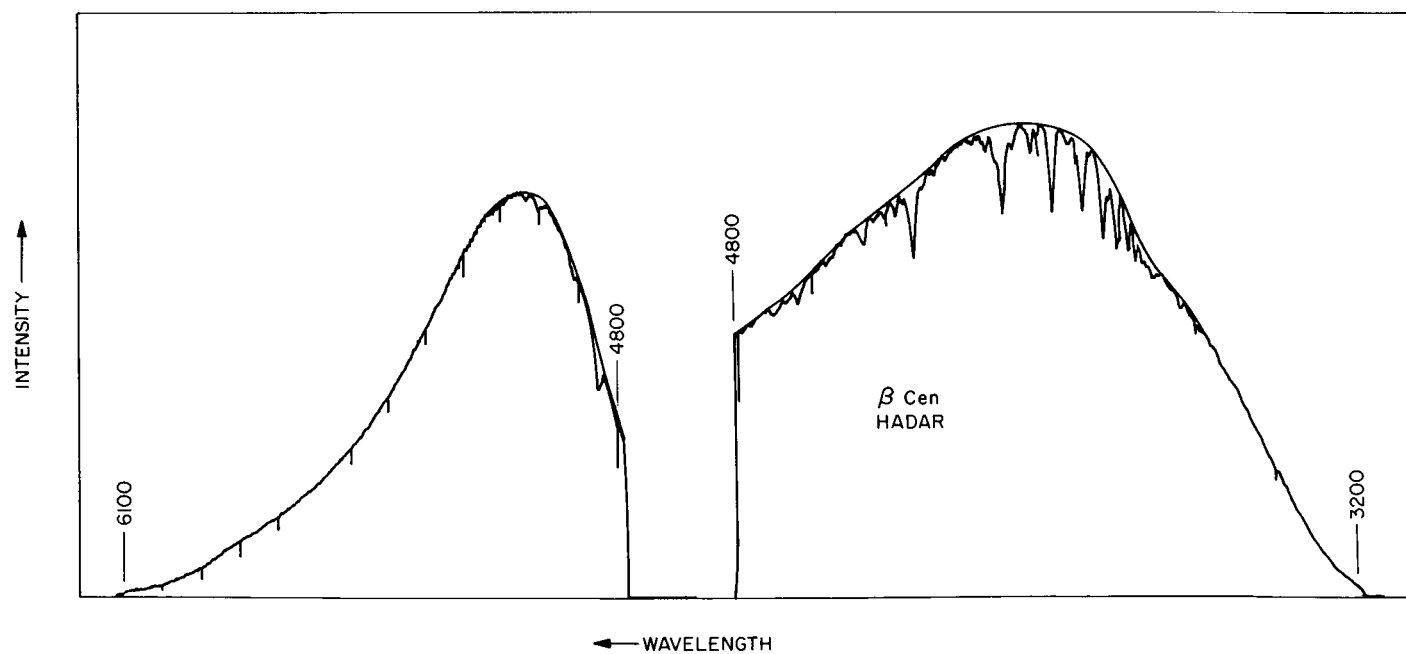


Fig. B-7. Reproduction of actual scanner tracing

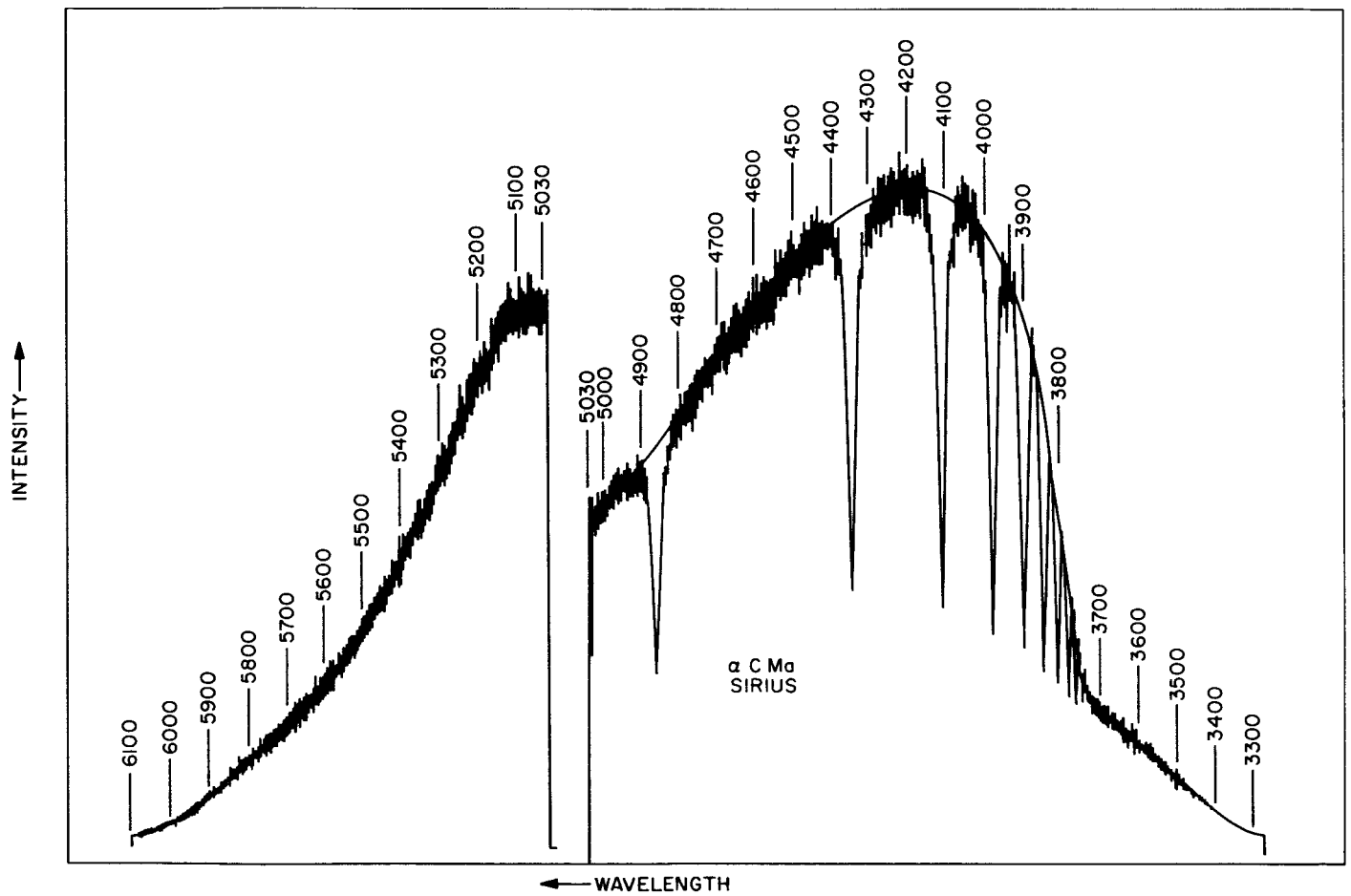


Fig. B-8. Reproduction of actual scanner tracing



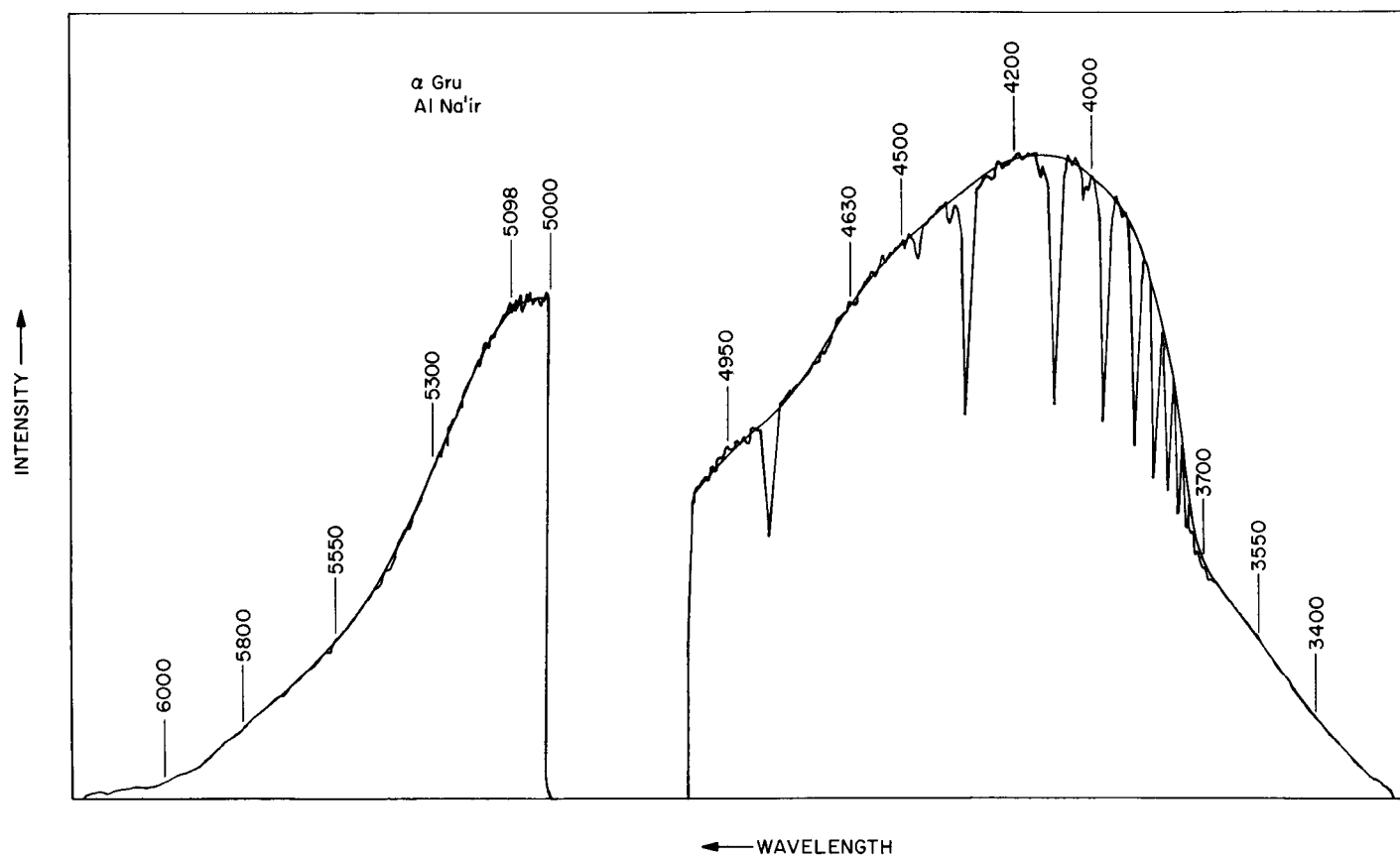


Fig. B-9. Reproduction of actual scanner tracing

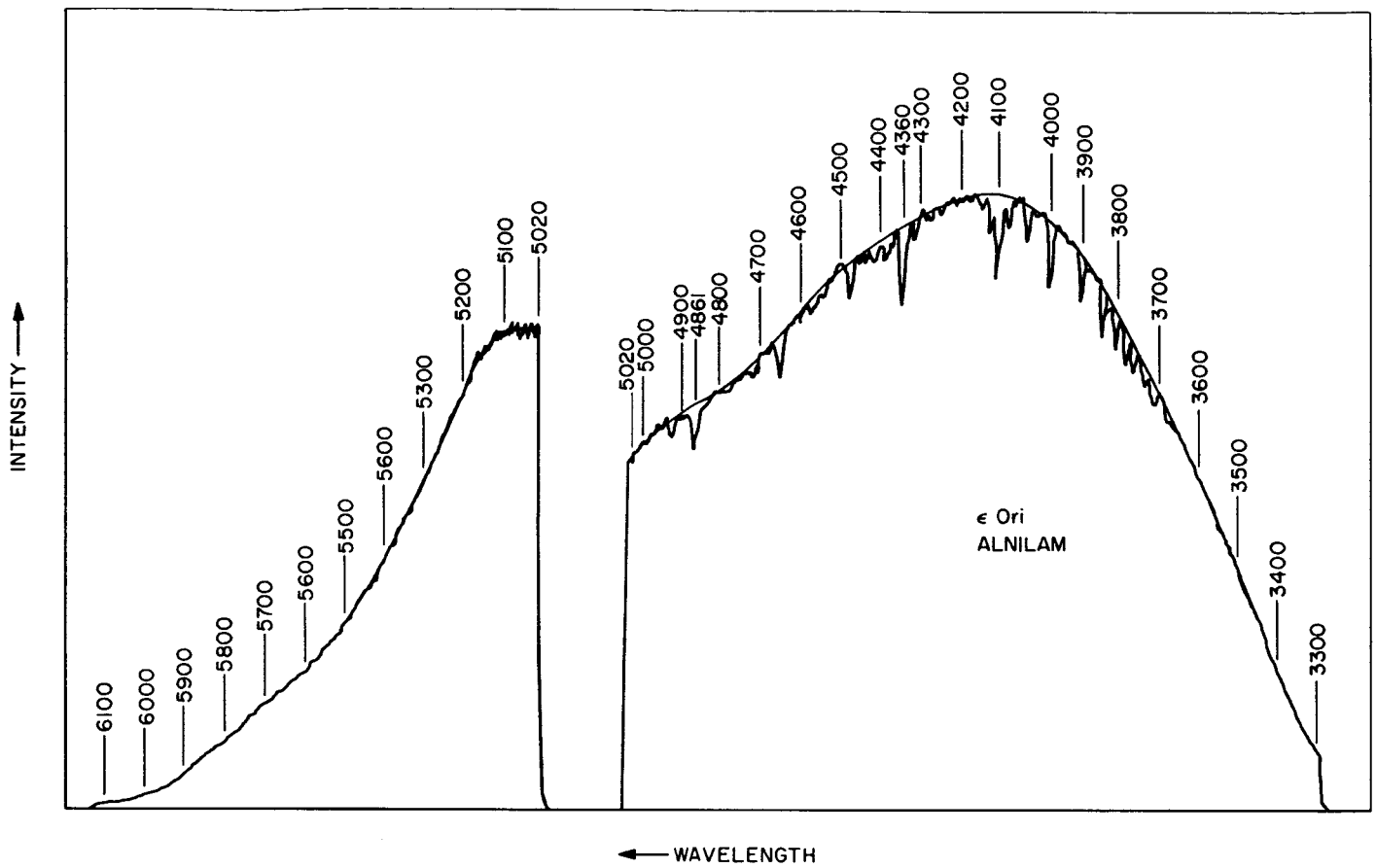


Fig. B-10. Reproduction of actual scanner tracing

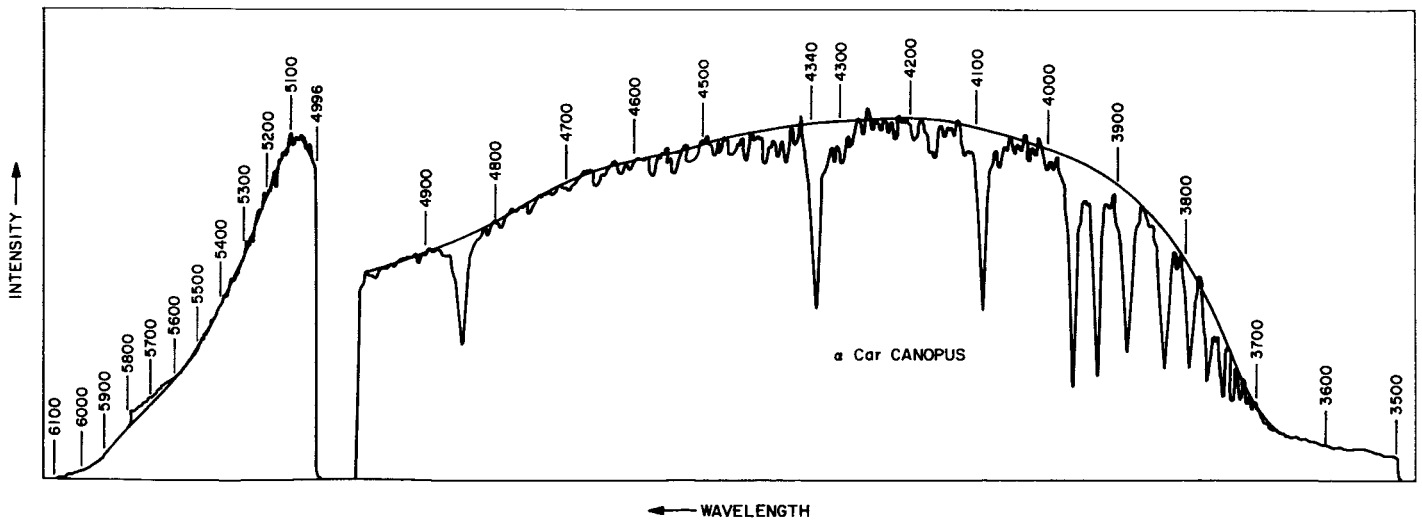


Fig. B-11. Reproduction of actual scanner tracing